



Co-funded by the
Erasmus+ Programme
of the European Union



**Erasmus+ Programme Key Action 2 Cooperation Partnerships
for Higher Education (KA220-HED)
Agreement number 2023-1-RO01-KA220-HED-000155412
*European Network for Additive Manufacturing in Industrial
Design for Ukrainian Context***

IO3 – AMAZE VR/AR e-learning platform for virtual laboratory

Project Title	European Network for Additive Manufacturing in Industrial Design for Ukrainian Context 2023-1-RO01-KA220-HED-000155412
Output	Additive Manufacturing of metallic complex lattices used in industry
Date of Delivery	September 2024
	National University of Science and Technology Politehnica Bucharest
Version	FINAL VARIANT, *14.09.2024

This project has been funded with support from the Erasmus+ Programme Key Action 2 Cooperation Partnerships for Higher Education (KA220-HED). This publication [communication] reflects the views only of the authors, and the Commission cannot be held responsible for any use which may be made of the information contained therein.



1. Introduction

The main AM technologies recognized and used today are differentiated according to the nature of the raw material, the post-processing operations required to be carried out, the physical-mechanical properties of the manufactured models. All these technologies are integrated CAD/CAM systems. [1-4] The most important are:

- 3D Printing;
- 3D Bioprinting;
- LOM (Laminated Object Manufacturing);
- FDM (Fused Deposition Modeling);
- SLA (Stereolithography);
- DLP (Digital Light Processing);
- Polyjet Printing;
- SLS (Selective Laser Sintering);
- DMLS (Direct Metal Laser Sintering);
- LENS (Laser Engineered Net Shaping);
- SLM (Selective Laser Melting);
- EBM (Electron Beam Melting);
- Stratoconception;
- RFP (Rapid Freeze Prototyping);
- UC (Ultrasonic Consolidation).

As part of the experimental research, different functional prototypes of some 3D parts were made. The 3D printer used in the research was: Zmorph 2.0 SX (FDM technology).

The Zmorph 2.0 ZX - 3D printer (fig. 1) is a modern, state-of-the-art printer that produces parts with an accuracy of 25-300 microns. It is equipped with five heads: simple extruder, dual extruder, laser extruder (P=2mW), CNC head and ceramic deposition head, as in Figures1-3. The software used is Voxelizer. The file types used are STL, or gcode.

This project has been funded with support from the Erasmus+ Programme Key Action 2 Cooperation Partnerships for Higher Education (KA220-HED). This publication [communication] reflects the views only of the authors, and the Commission cannot be held responsible for any use which may be made of the information contained therein.



Co-funded by the
Erasmus+ Programme
of the European Union

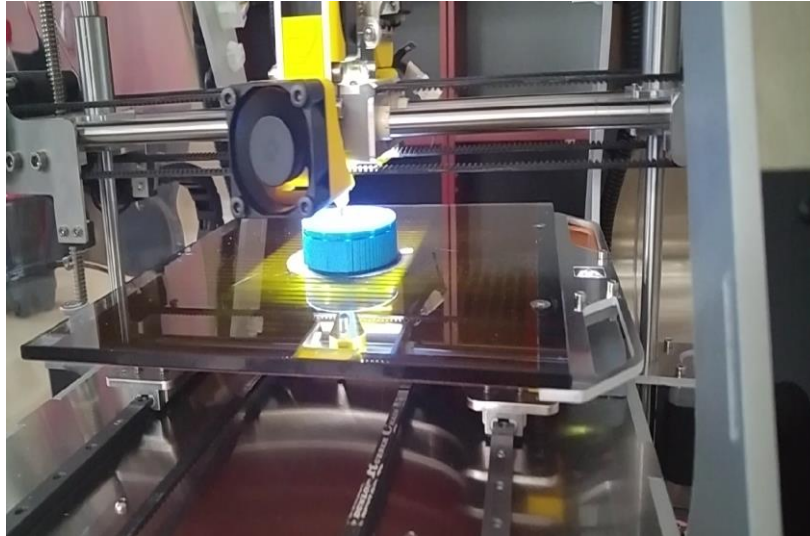


Fig.1. 3D printer – Zmorph 2.0 ZX

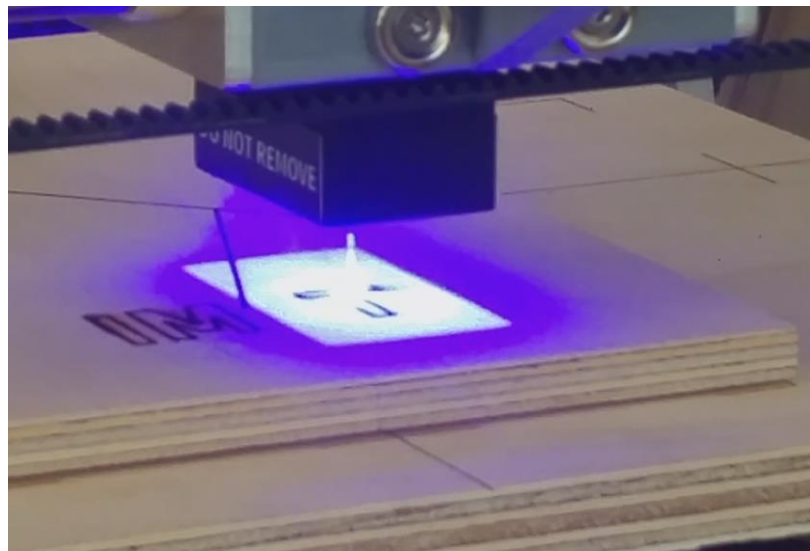


Fig.2. Laser engraving using Zmorph – 3D printer

This project has been funded with support from the Erasmus+ Programme Key Action 2 Cooperation Partnerships for Higher Education (KA220-HED). This publication [communication] reflects the views only of the authors, and the Commission cannot be held responsible for any use which may be made of the information contained therein.



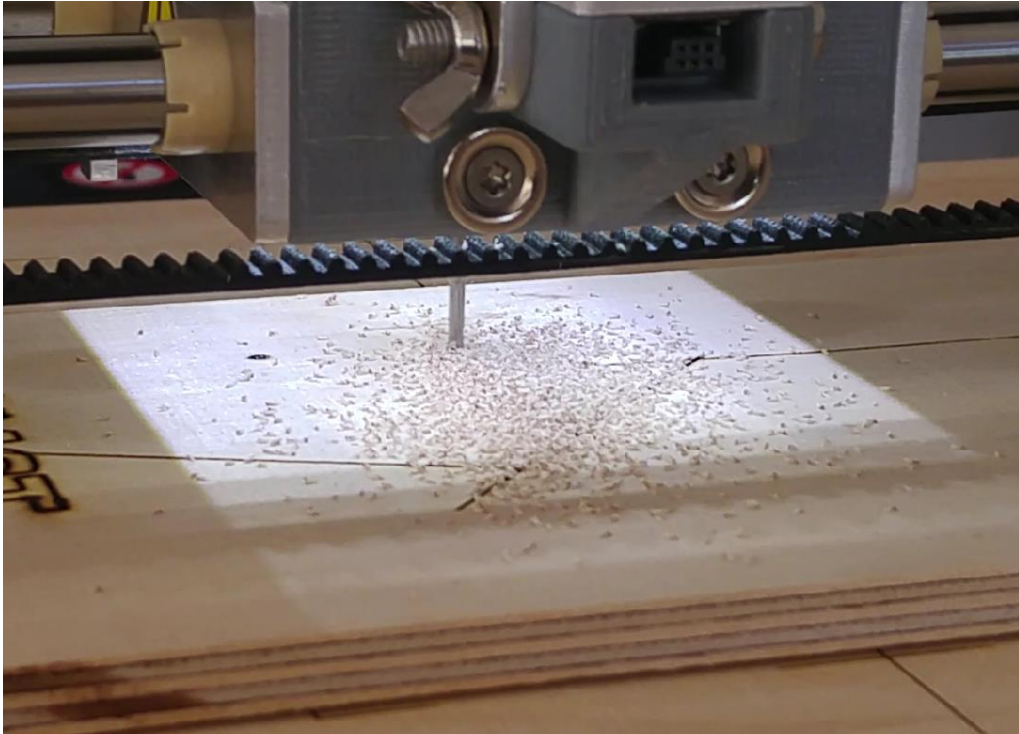


Fig.3. CNC machining using Zmorph – 3D printer

Properties of 3D printing of PLA material:

- Melting point: 190 °C;
- Printing temperature: 190-230°C
- High print speed: 40-100 mm/s
- Tolerance: ± 0.02 mm
- Heating bed temperature: without heated bed or with heated bed at 40-60°C
- Diameter: 1.75/2.85 mm;
- Total roll weight: 1.35 kg;
- Filament weight: 1 kg;

This project has been funded with support from the Erasmus+ Programme Key Action 2 Cooperation Partnerships for Higher Education (KA220-HED). This publication [communication] reflects the views only of the authors, and the Commission cannot be held responsible for any use which may be made of the information contained therein.



Co-funded by the
Erasmus+ Programme
of the European Union



- Different colors
- Thin layers deposited by 3D printing.
- Insoluble
- Limited flexibility
- Good durability
- Good resistance
- Good impact resistance
- Can be used in food.
- Small shrinkage during cooling, less sensitive compared to ABS
- Ideal for consumer products, small toys, faster print speeds, finer layers
- Printing difficulty is easy once the temperature, bed height and speed are set
- It is recyclable.

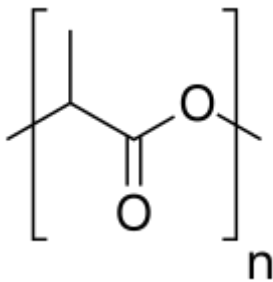


Table 1. Mechanical properties of PLA [5]

Properties	Units	Value
Melting Point	°C	190-220
Density	g/cm ³	1.20-1.25
Diameter of Filament	mm	1.75
Tensile Yield Strength	MPa	62.63
Elongation at Break	%	4.43
Flexural Strength	MPa	65.02
Flexural Modulus	MPa	2504.4
Impact Strength	KJ/m ²	4.28

This project has been funded with support from the Erasmus+ Programme Key Action 2 Cooperation Partnerships for Higher Education (KA220-HED). This publication [communication] reflects the views only of the authors, and the Commission cannot be held responsible for any use which may be made of the information contained therein.





2. Experimental part

The guide-support was designed using SolidWorks software, having the dimensions specified in Figure 4.

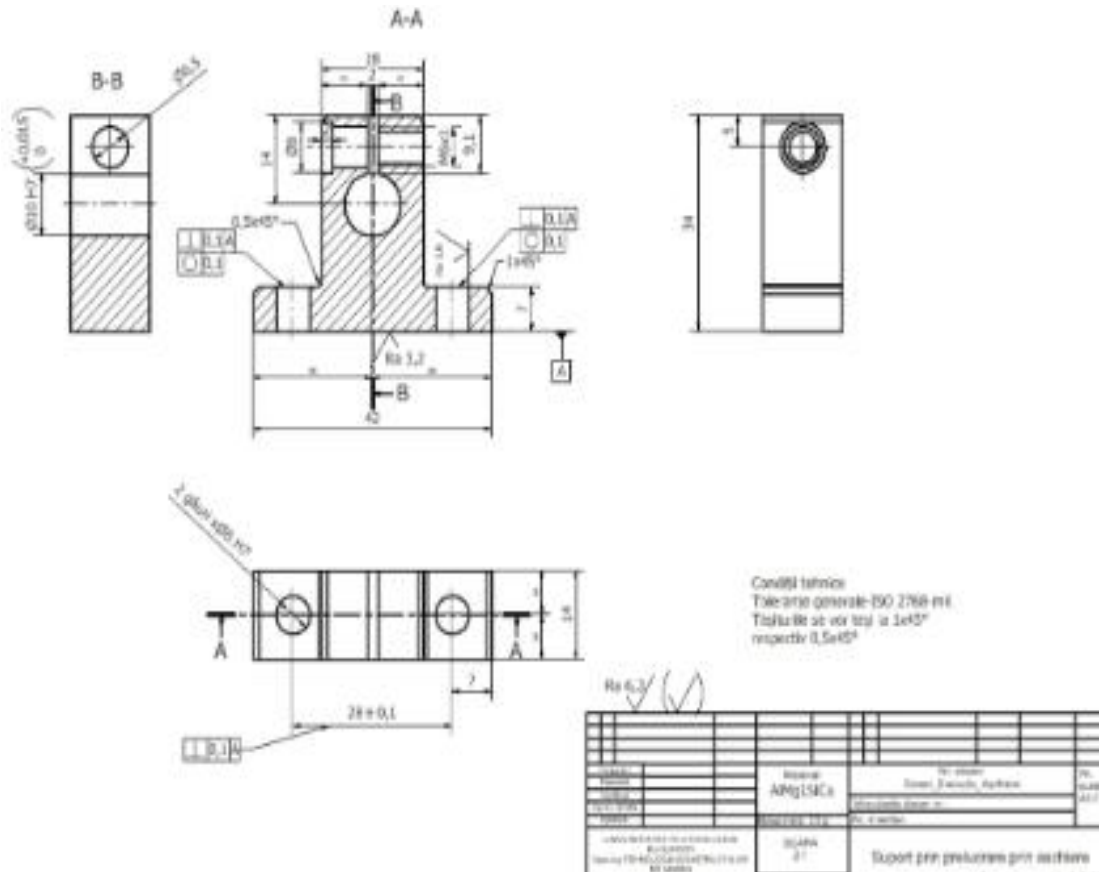


Fig.4. The guide support

In Figure 5 are presented the necessary steps for guide support design, the STL file. In Figure 6 was realized the gcode file for 3D Printing process. The manufacturing parameters for 3D Printing of the guide support, were indicated by the Voxelizer software, such in Figure 7.

This project has been funded with support from the Erasmus+ Programme Key Action 2 Cooperation Partnerships for Higher Education (KA220-HED). This publication [communication] reflects the views only of the authors, and the Commission cannot be held responsible for any use which may be made of the information contained therein.



In case, the thickness of the deposited layer is 0.09 mm, the material used is PLA, and the filament melting temperature in the extruder is between 200-220°C. The table is heated up to 20°C during manufacturing. For efficient cooling of the deposited layer, 1 cooler is used. The generation of g-code is carried out for 3D printing. In the case of guide support, the piece will have 181 layers, the layer thickness is 0.09 mm, 1.80 m of PLA filament will be used, and the 3D printing time will be approximately 1 hour and 13 minutes. The 3D printed part by FDM technology is shown in fig.9. The cost of a roll of PLA filament is 20 \$.

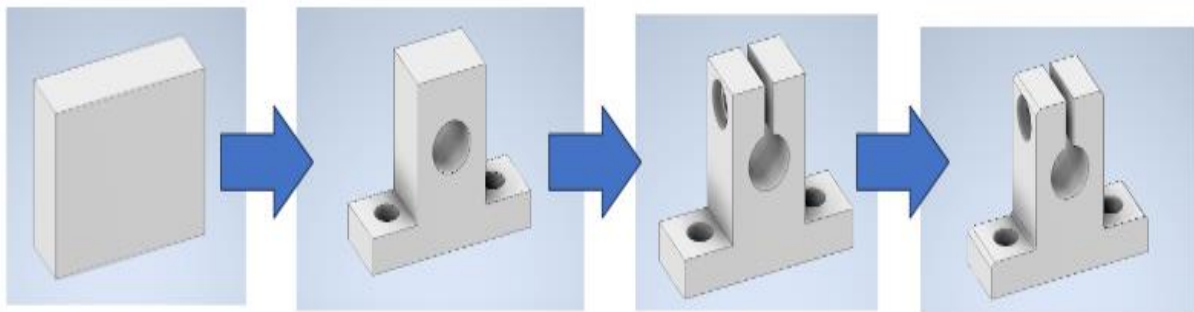


Fig.5. Necessary Steps for guide support design – STL file

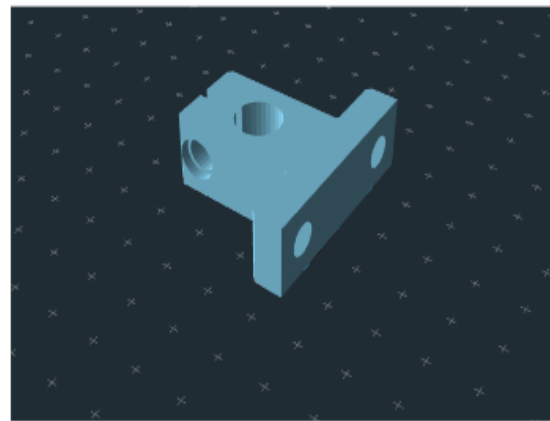
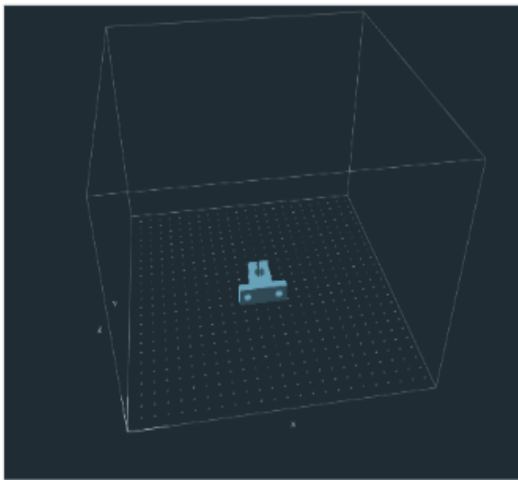


Fig.6. Gcode of guide support using Voxelizer software

This project has been funded with support from the Erasmus+ Programme Key Action 2 Cooperation Partnerships for Higher Education (KA220-HED). This publication [communication] reflects the views only of the authors, and the Commission cannot be held responsible for any use which may be made of the information contained therein.

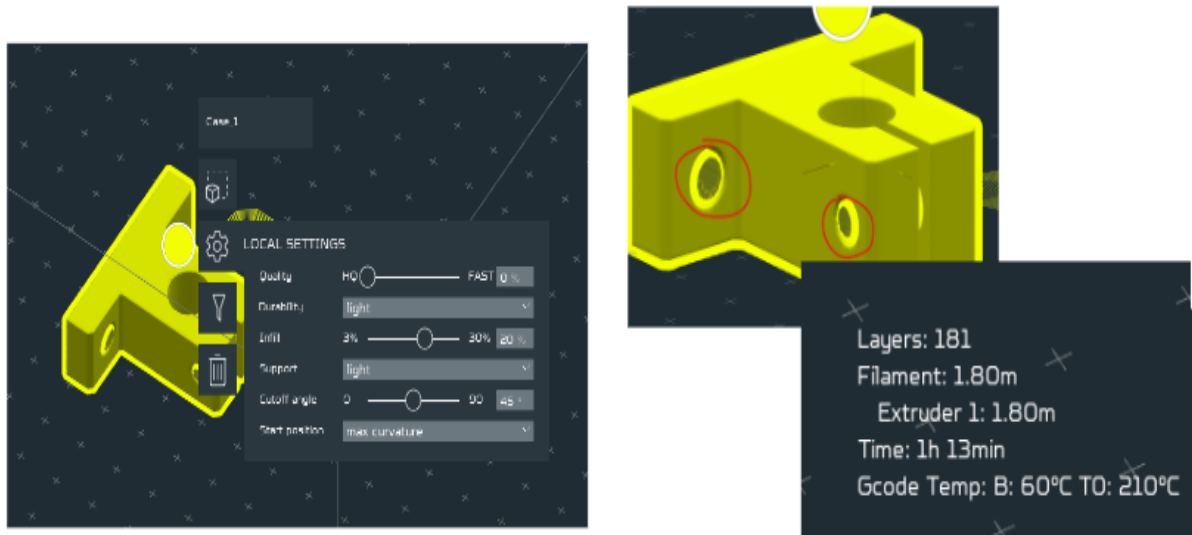


Fig.7. Manufacturing parameters for 3D Printing of the guide support



Fig.8. Printed guide support

In Figure 8 shows the printed guide support and the FEA simulations are realized using SolidWorks software as in Figure 9, and can remark the stresses and the displacements.

This project has been funded with support from the Erasmus+ Programme Key Action 2 Cooperation Partnerships for Higher Education (KA220-HED). This publication [communication] reflects the views only of the authors, and the Commission cannot be held responsible for any use which may be made of the information contained therein.

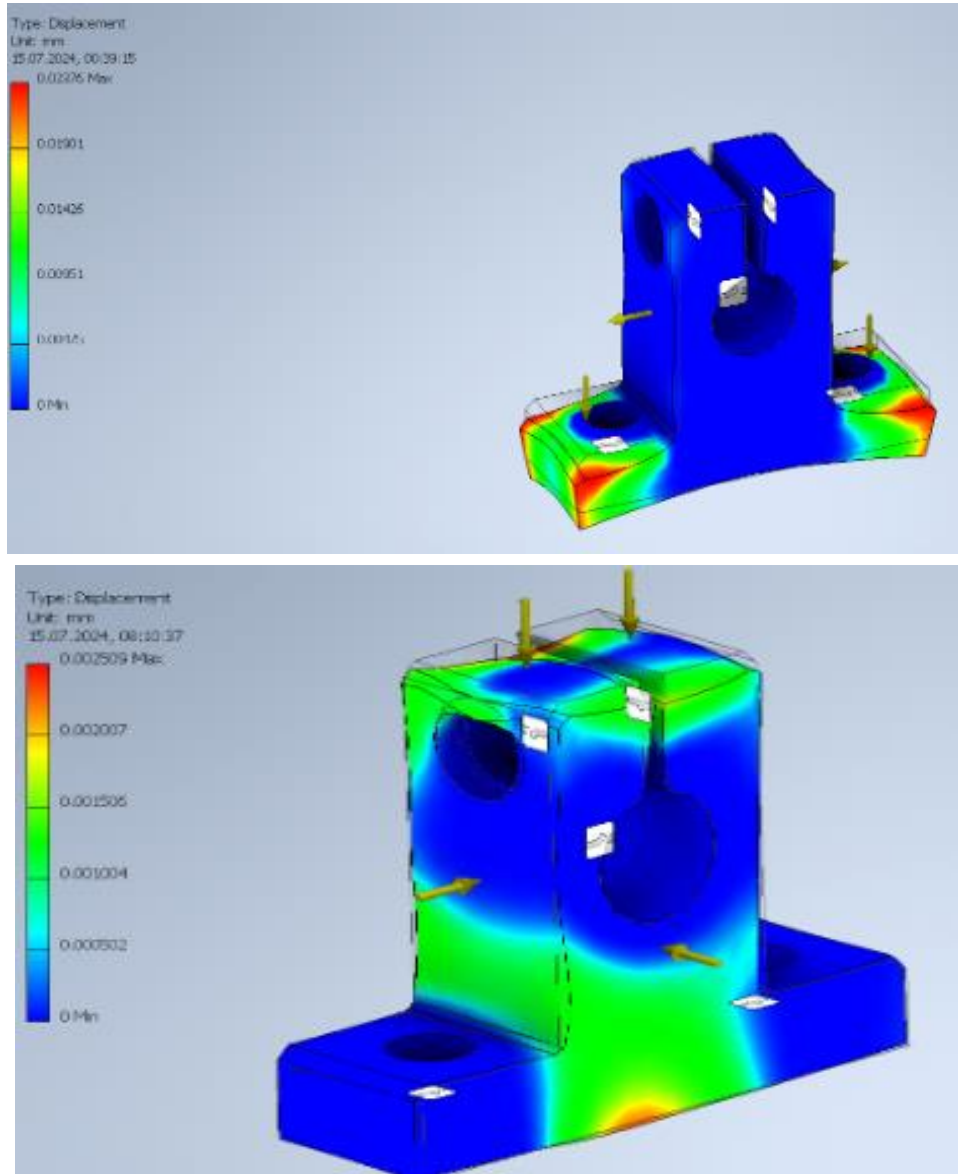


Fig.9. FEA simulation for guide support

This project has been funded with support from the Erasmus+ Programme Key Action 2 Cooperation Partnerships for Higher Education (KA220-HED). This publication [communication] reflects the views only of the authors, and the Commission cannot be held responsible for any use which may be made of the information contained therein.



The phone case was designed using the software SolidWorks, having the dimensions specified in Figure 10. The design details of phone case are presented in Figures 11 and 12.

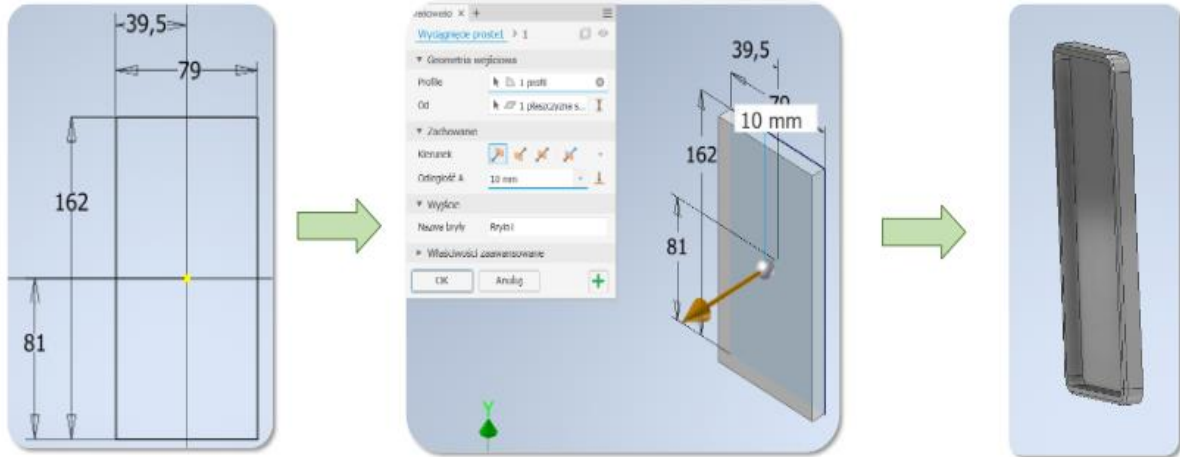


Fig.10. Phone case dimensions

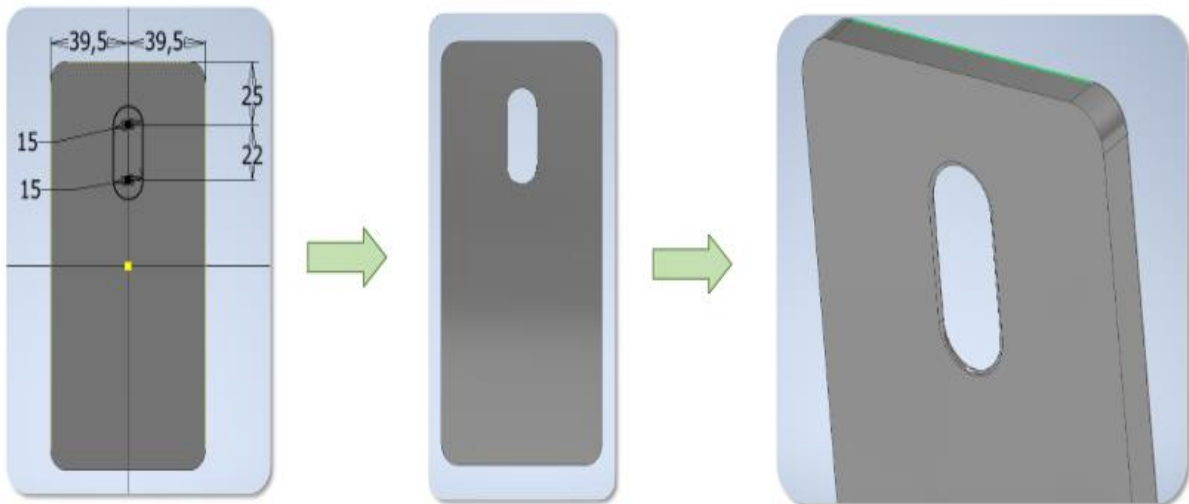


Fig.11. Design of the phone case

This project has been funded with support from the Erasmus+ Programme Key Action 2 Cooperation Partnerships for Higher Education (KA220-HED). This publication [communication] reflects the views only of the authors, and the Commission cannot be held responsible for any use which may be made of the information contained therein.



Co-funded by the
Erasmus+ Programme
of the European Union

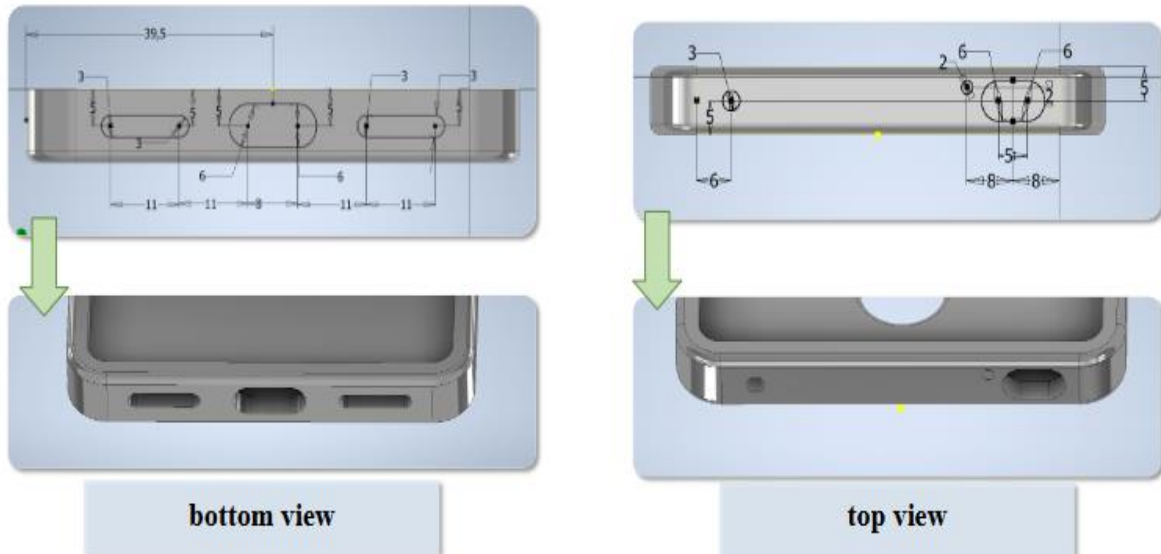


Fig.12. Design details of the phone case

In Figure 13 is shown the STL file of the phone case.



Fig.13. STL file of the phone case

This project has been funded with support from the Erasmus+ Programme Key Action 2 Cooperation Partnerships for Higher Education (KA220-HED). This publication [communication] reflects the views only of the authors, and the Commission cannot be held responsible for any use which may be made of the information contained therein.



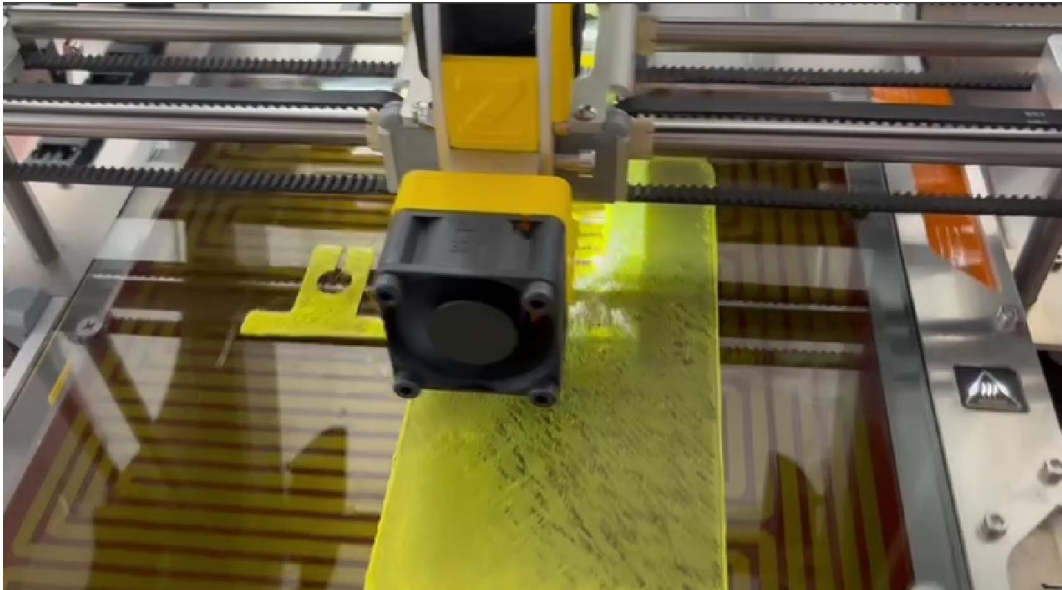


Fig.14. 3D Printing process of phone case and guide support

Defects of the phone case, printed by FDM technology are presented in Figure 15:

- uneven edges
- too little filling
- thin walls
- too much material on the edges

Improvements:

- more filling
- setting the right print parameters
- precise calibration of the printer
- not moving the printer table while printing

This project has been funded with support from the Erasmus+ Programme Key Action 2 Cooperation Partnerships for Higher Education (KA220-HED). This publication [communication] reflects the views only of the authors, and the Commission cannot be held responsible for any use which may be made of the information contained therein.



Fig.15. Defects of the phone case, printed by FDM technology

Finite Element Analysis (FEA) for the phone case is presented in Figure 16, and the stresses and displacements are presented on the phone case, as in Figure 17.



Fig.16. FEA simulation for the phone case

This project has been funded with support from the Erasmus+ Programme Key Action 2 Cooperation Partnerships for Higher Education (KA220-HED). This publication [communication] reflects the views only of the authors, and the Commission cannot be held responsible for any use which may be made of the information contained therein.

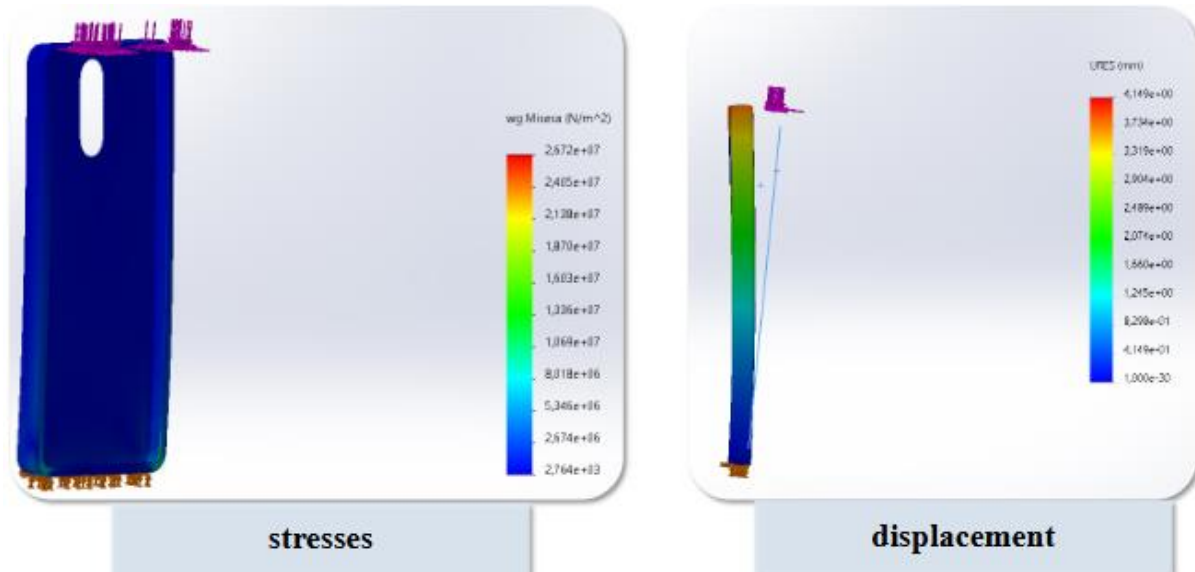


Fig.17. Stresses and displacements on FEA simulation for the phone case

3.Conclusions

The models obtained through Additive Manufacturing optimize the design of a new model or the modernization of an existing one, these models allow the physical visualization of the product and improve the communication between the manufacturer and the beneficiary. The models manufactured by these new technologies can be used for various test modes, the most implemented of which are:

- functional tests;
- simulation tests;
- control tests;
- manufacturing tests;
- fastening and assembly tests;
- packaging tests.

Testing a product manufactured by Additive Manufacturing technologies depends on three factors material, size and design. The tests carried out must lead to a visual acceptance, an

This project has been funded with support from the Erasmus+ Programme Key Action 2 Cooperation Partnerships for Higher Education (KA220-HED). This publication [communication] reflects the views only of the authors, and the Commission cannot be held responsible for any use which may be made of the information contained therein.





Co-funded by the
Erasmus+ Programme
of the European Union



understanding of the construction, the functionality of the product and the finalization of the dimensioning elements.

Additive Manufacturing technologies have an important role in many industrial fields as: electronics, automotive, tooling, medicine, aeronautical and aerospace, architecture, and jewelry, thus giving the technology a strategic importance for the companies that use these technologies.

All 3D printed parts and their design were realized with the students participating at the Summer School, hosted by National University of Science and Technology Politehnica Bucharest, Romania, from 8-17 July 2024, on AMAZE project.

References:

1. Berce P.&others - Tehnologii de fabricație prin adăugare de material și aplicațiile lor - Editura Academiei Române, București 2014;
2. Ratner Buddy D., Hoffman Allan S., Schoen Frederick J., Lemons Jack E.- Biomaterials Science, An introduction to materials in medicine –Academic Press, 2013;
3. Earle J. – Graphics for engineers, 5th edition, Pretince-Hall, 1999, ISBN 0130160075;
- 4.<https://zmorph3d.com/>
5. Dave, H.K., Rajpurohit, S.R., Patadiya, N.H., Dave, S.J., Kumar, S., Sharma, Thambad, S.S., Srinivasn, V.P., & Sheth. Compressive strength of PLA based scaffolds: effect of layer height, infill density and print speed, International Journal of Modern Manufacturing Technologies ISSN 2067–3604, Vol. XI, No. 1, 2019.

This project has been funded with support from the Erasmus+ Programme Key Action 2 Cooperation Partnerships for Higher Education (KA220-HED). This publication [communication] reflects the views only of the authors, and the Commission cannot be held responsible for any use which may be made of the information contained therein.





Co-funded by the
Erasmus+ Programme
of the European Union



Morphology and design of lattice structures manufactured by SLM (Selective Laser Melting) using different metallic powders

The laser powder bed fusion technologies is formed by SLM (Selective Laser Melting), DMLS (Direct Metal Laser Sintering), and EBM (Electron Beam Melting) technologies, and are used for parts with fine details, with a high degree of complexity of shapes, and with good mechanical properties. [1-5] The melting process of the metallic powders is realized using a concentrated laser with a high power, and for the design part is used a CAD/CAM software. In the Selective Laser Melting, the sintered structure of the parts presents a porous structure, but the quality of this, can be affected by many defects as lack of fusion, cracking within solidified regions, balling phenomenon due of the particle's dynamics in contact with the laser beam.

Selective Laser Melting process uses fine-grained powder between 5-30 microns of Co-Cr, Inconel 625, Inconel 718, Ti-6Al-4V, Ti pure, etc. , which is selectively melted layer by layer to obtain the 3D products. The granulometry of the raw metallic powders influence the accuracy of Selective Laser Manufacturing. [6-10]

Balbaa M. studied the selective laser melting of Inconel 718, concerning the densification, surface roughness and residual stresses induced into sintered material during the manufacturing process. [3]

Dahiya U.R. considers Nitinol is a versatile metallic alloy, with a shape memory effect, and that it is used frequently in different applications for biomedical devices and implants. [11]

The Selective Laser Melting process takes place in an inert atmosphere, shielding gas, such as nitrogen or argon, to avoid metal oxidation. The shielding gas influences too, the quality of the manufactured sintered parts. Like all laser additive manufacturing technologies, selective laser melting allows the creation of parts with fine details and high precision leading to great geometric freedom, as presents Fu W. [12]

This means that extremely complex geometries and various customized medical prostheses, or various manufactured parts from the dental, cardiology (Gerontas A., Guerra J.A., Hoare D.) [13-16], aeronautical, aerospace or automotive fields, which were practically impossible to achieve with traditional manufacturing technologies, can be created with SLM technology. Technology Selective Laser Melting is used to produce different industrial and medical prototypes. Selective Laser Melting of metal powders (SLM) must hold account of 4 dates: temperature profile; the thermal gradient of the metal powder; speed of solidification; speed of cooling. For large series production, Selective Laser Meting systems used laser powers of

This project has been funded with support from the Erasmus+ Programme Key Action 2 Cooperation Partnerships for Higher Education (KA220-HED). This publication [communication] reflects the views only of the authors, and the Commission cannot be held responsible for any use which may be made of the information contained therein.



1kW. SLM manufacturing systems use different sources regarding the 3D model, namely: - convert CAD files (*STEP, *IGES); -3D scan (optical, XR,...) of the existing model. -3D models designed and exported from various design software (Blender, Catia, Solid Works, ProEngineer, Inventor, OnShape, etc.), saved as *stl or *gcode files. [17-19]

Leary M. researched in his article, Inconel 625 lattice structures manufactured by Selective Laser Melting (SLM), concerning mechanical properties, deformation and failure nodes, realizing different Inconel 625 lattice structures with a robust design. [17]

Mc Gee carried out an investigation into patient-specific 3D printed titanium stents and the use of etching to overcome Selective Laser Melting design constraints and testing different stents' performance using patient-specific finite element models. Titanium and his alloys are biocompatible materials, and present very good mechanical properties. [20]

It is noted that the most used technologies in the field of Additive Laser Manufacturing are the DMLS/SLM technologies, there are most of them on the market manufacturing systems of this type. The dimensions of the parts manufactured by DMLS/SLM technologies are quite limited, with only parts of small, medium sizes. The manufacturing time of DMLS/SLM technologies is relatively large. The quality and precision of the surfaces obtained by these technologies are very good, obtaining lacy and fine structures. [21,22]

The parts manufactured by SLM are characterized by a particularly high density, in rapport with other technologies as, SLS (Selective Laser Sintering) or DMLS (Direct Metal Laser Sintering) technology and almost pore-free surfaces, grace of the greater power laser. Mechanical properties and fatigue strength of parts manufactured by technologies are quite good, obtaining results similar to parts forged. [23,24]

In this article, the novelty was to design different types of lattice structures, from different metallic powders, as Ti-6Al-4V, and Inconel, and these powders were examined by SEM, EDAX, and Mapping analysis. Other objective of this article was to determine the morphology structure, XRD analysis and Mapping analyses were established for Ti-6Al-4V and 625 Inconel lattice structures manufactured by SLM.

2 Experimental part

For the selective laser melting (SLM) of the Ti-6%Al-4%V alloy, an SLM manufacturing system was used - type Lasertec 30 SLM (DMG MORI) which has a laser power of 600W, Ytterbium YLR fiber laser -6000-WC, a wavelength of 1070 ± 10 nm, layer thickness between 20-100 μ m, construction volume being 300x300x300 mm. Materials processed are tool steel, stainless

This project has been funded with support from the Erasmus+ Programme Key Action 2 Cooperation Partnerships for Higher Education (KA220-HED). This publication [communication] reflects the views only of the authors, and the Commission cannot be held responsible for any use which may be made of the information contained therein.

steel, superalloy Co-Cr, Inconel, Ti, Al and precious metals. In this article, the lattice structures of Ti-6Al-4V, respectively 625 Inconel were designed and made by selective laser melting with a great power laser, using a 50 μm layer print was used, as in Figure 1.

The metallic powders of Ti-6Al-4V, and 718 and 625 Inconel were studied in this article.

The SEM (scanning electron microscopy), EDS (energy-dispersive X-ray spectroscopy) analysis and mapping analysis of the samples made of metallic materials were performed using a scanning electron microscope QUANTA INSPECT F50 type with a field emission gun (FE-SEM) (Thermo Fisher, Eindhoven, Netherlands) and a resolution of 1.2 nm, coupled with an energy-dispersive X-ray spectrometer (Thermo Fisher, Eindhoven, Netherlands) with a resolution of 133 eV at MnK. The areas of interest which were analysed qualitatively on the top surface and side surface of the realized samples made of metallic materials, as well on the surface of the samples, were analyzed qualitatively by microcompositional X-ray spectrometry and obtained spectra were plotted using ImageJ 1.50i software (Wayne Rasband National Institute of Health, 2016, MD, USA). For SEM analysis, the specimens were cleaned with distilled water and isopropyl alcohol.

Other methods of analysis of the Ti-6Al-4V sample, manufactured by SLM were: X-ray fluorescence spectroscopy, X-ray structural analysis, and hydrostatic weighing.

The devices used, were: precision analyser Expert 3L (X-ray diffractometer Shimadzu XRD-7000), scales for hydrostatic weighing.

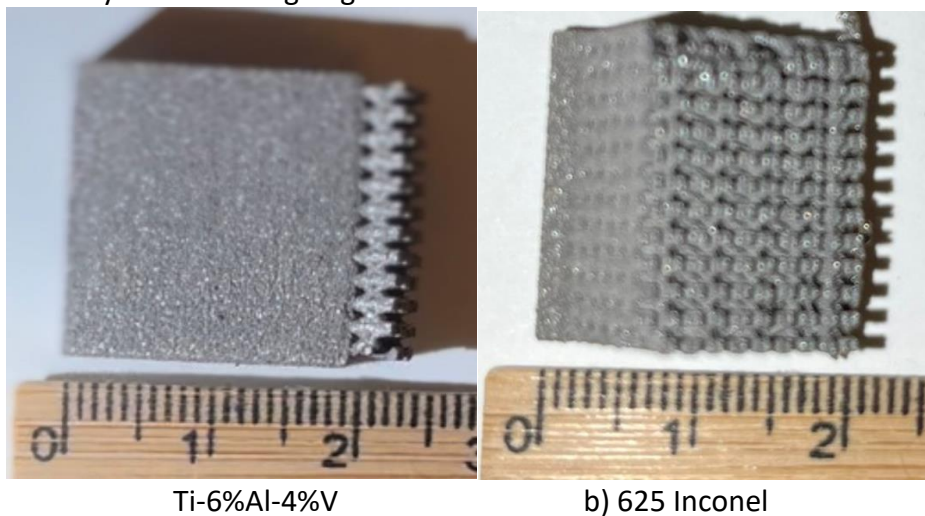


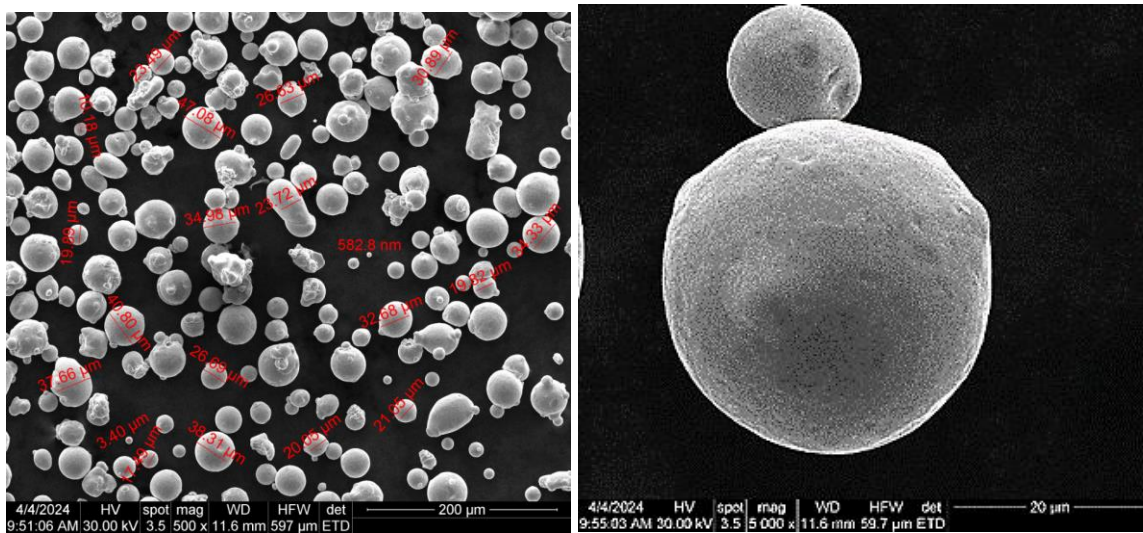
Fig.1. Lattice structures of Ti-6%Al-4%V a), respectively 625 Inconel b) - obtained by SLM

This project has been funded with support from the Erasmus+ Programme Key Action 2 Cooperation Partnerships for Higher Education (KA220-HED). This publication [communication] reflects the views only of the authors, and the Commission cannot be held responsible for any use which may be made of the information contained therein.



3 Experimental research concerning the morphology and properties of Inconel 625, Inconel 718, Co-Cr and Ti6Al4V powders used in Selective Laser Melting

One of our research consists of the experimental comparison of metal powders (Ti6Al4V, Inconel 625 and Inconel 718) used in Selective Laser Melting. Inconel 625 metal powder is a superalloy containing Ni, Cr, Fe, Mo, and Nb. The melting temperature is between 1290-1350°C, the electrical resistivity of $129 \mu\Omega \cdot \text{cm}$ (21°C), the tensile strength of 827-1034 MPa, and the thermal conductivity of $9.8 \text{ W/m} \cdot ^\circ\text{C}$ (21°C). The granulometry of the Inconel 625 superalloy is very fine, as in Figure 2, the powder grains have a spherical shape, and the diameter of the grains is of the order of microns, varying between 0.582 – 40.8 μm .

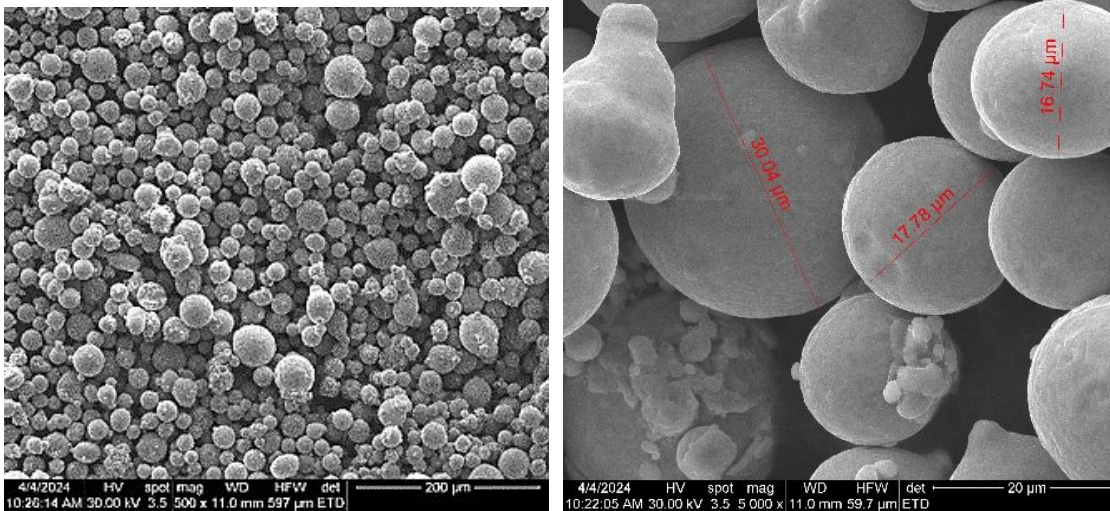


X500

(b) X5000

Figure 2. SEM analysis of superalloy powder - Inconel 625:
a) X500; b) X5000

This project has been funded with support from the Erasmus+ Programme Key Action 2 Cooperation Partnerships for Higher Education (KA220-HED). This publication [communication] reflects the views only of the authors, and the Commission cannot be held responsible for any use which may be made of the information contained therein.



(a) X500

(b) X5000

Figure 3. SEM analysis for superalloy powder - Inconel 718:
a)X500; b) X5000

Inconel 718 type metal powder is a superalloy containing Ni, Cr, Fe. The melting temperature is between 1370-1430°C, density 8.192 g/cm³, electrical resistivity of 129 μΩ*cm (21°C), tensile strength of 827-1034 MPa, thermal conductivity of 6.5W/m*°C (21°C). The granulometry of the Inconel 718 superalloy is also very fine, as in Figure 3, the powder grains have a spherical shape, specific to the powders intended for the manufacture of SLM, and the diameter of the grains is of the order of microns, varying between 4.43 -32.85 μm. The applications of Inconel superalloys are in additive manufacturing, the aerospace industry, aeronautics, the automotive industry, metallurgy, the military field, and research. Table 1 shows the chemical composition of Inconel 625 and Inconel 718 type superalloys.

Table 1. Chemical composition of the Inconel superalloy [28]

Inconel alloy	Element (mass percentage)														
	Ni	Cr	Fe	Mo	Nb	Co	Mn	Cu	AL	Ti	Si	C	S	P	B
625		58.0	20.0-23.0	5.0	8.0-10.0	3.15-4.15	1.0	0.5		0.4	0.4	0.5	0.1	0.015	
718		50.0-55.5	17.0-21.0		2.8-3.3	4.75-5.5	1.0	0.35	0.2-0.8	0.65-1.15	0.3	0.35	0.08	0.015	0.006

This project has been funded with support from the Erasmus+ Programme Key Action 2 Cooperation Partnerships for Higher Education (KA220-HED). This publication [communication] reflects the views only of the authors, and the Commission cannot be held responsible for any use which may be made of the information contained therein.



Ti-6Al-4V metal powder is an alloy containing Ti, 6%Al, and 4%V. The melting temperature is between 1604-1660°C, the density of 4.43g/cm³, the electrical resistivity of 178 μΩ*cm (21°C), the tensile strength of 950 - 1000 MPa, the thermal conductivity of 6.7 W/m*°C (21°C).

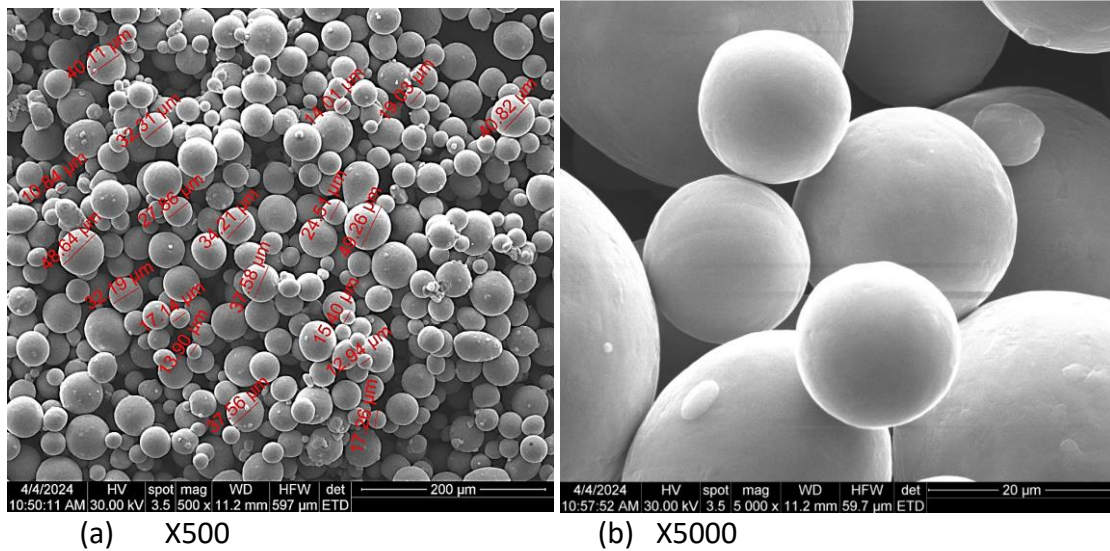


Figure 4. SEM analysis for alloy Ti-6Al-4V powder:
X500; b) X5000

The granulometry of the Ti-6Al-4V alloy is also very fine, as in Figure 4, the powder grains having a specific spherical shape obtained by atomization, and the diameter of the grains is of the order of microns, varying between 10-37 μm. The applications of Ti-6Al-4V alloy are in additive manufacturing, aeronautic and aerospace industry, automotive industry, medicine as a biomaterial, in research.

In the atomization process, the molten metal is separated into small droplets and quickly frozen before the droplets come into contact with each other or a solid surface. Typically, a thin stream of molten metal is disintegrated by subjecting it to the impact of high-energy jets of gas or liquid.

This project has been funded with support from the Erasmus+ Programme Key Action 2 Cooperation Partnerships for Higher Education (KA220-HED). This publication [communication] reflects the views only of the authors, and the Commission cannot be held responsible for any use which may be made of the information contained therein.

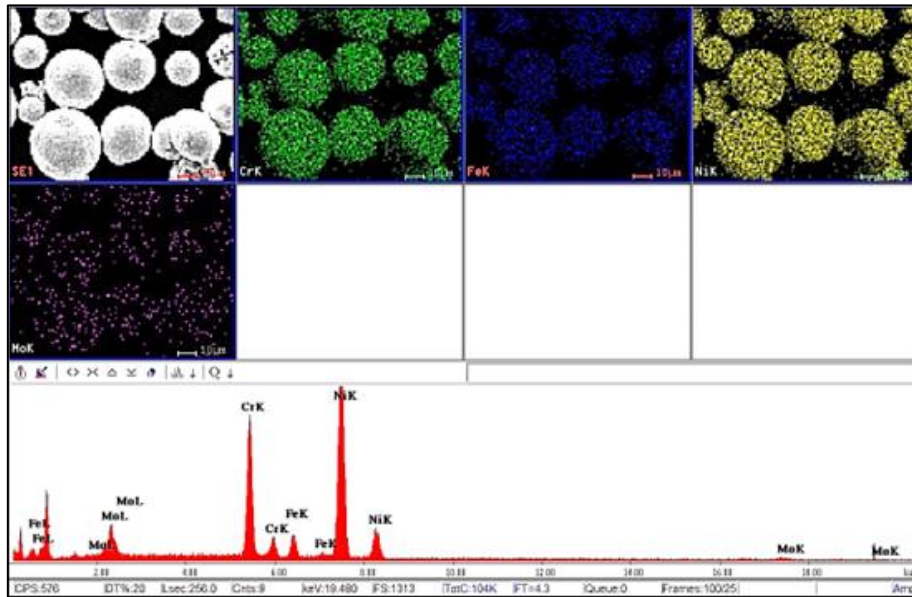


Figure 5. Mapping analysis of 625 Inconel

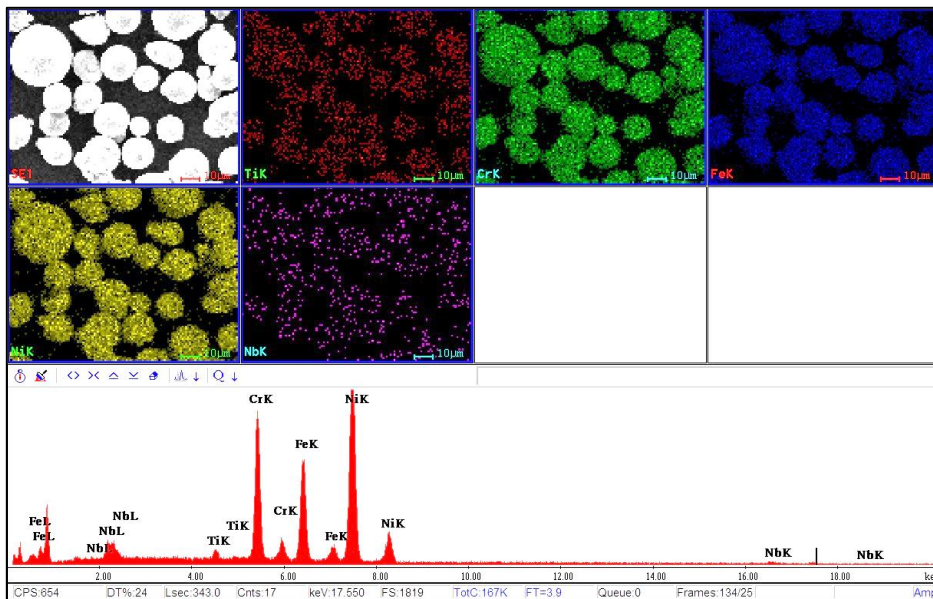


Figure 6. Mapping analysis of 718 Inconel

This project has been funded with support from the Erasmus+ Programme Key Action 2 Cooperation Partnerships for Higher Education (KA220-HED). This publication [communication] reflects the views only of the authors, and the Commission cannot be held responsible for any use which may be made of the information contained therein.



Metal powders can be obtained through the HDH process - hydride-dehydration, such as the Ti-6%Al-4%V powder, which is obtained due to the embrittlement phenomenon of Ti in the presence of hydrogen.

The other 625 Inconel and 718 Inconel powders can be obtained by gas atomization, plasma atomization, or the process with plasma electrode rotation. This explains the fact that we have particles with perfect spherical shapes in the case of Inconel 625 powder, because it was obtained by plasma atomization, as in Figure 5. The chemical elements distribution is uniform in all powder mass (Fe, Cr, Ni, Mo) as is shown in Figure 5. The Inconel 718 powder was obtained by gas atomization, the spherical shape of the grains can be noted, but there are also slightly deformed particles, as in Figure 6. The Mapping analysis of 718 Inconel presents an uniform distribution of the chemical compounds as Ti, Cr, Fe, Ni, Nb, as in Figure 6. Likewise, the EDAX analysis can be noted for the two Inconel superalloys and the uniformity of the distribution of chemical elements and the fineness of the powder.

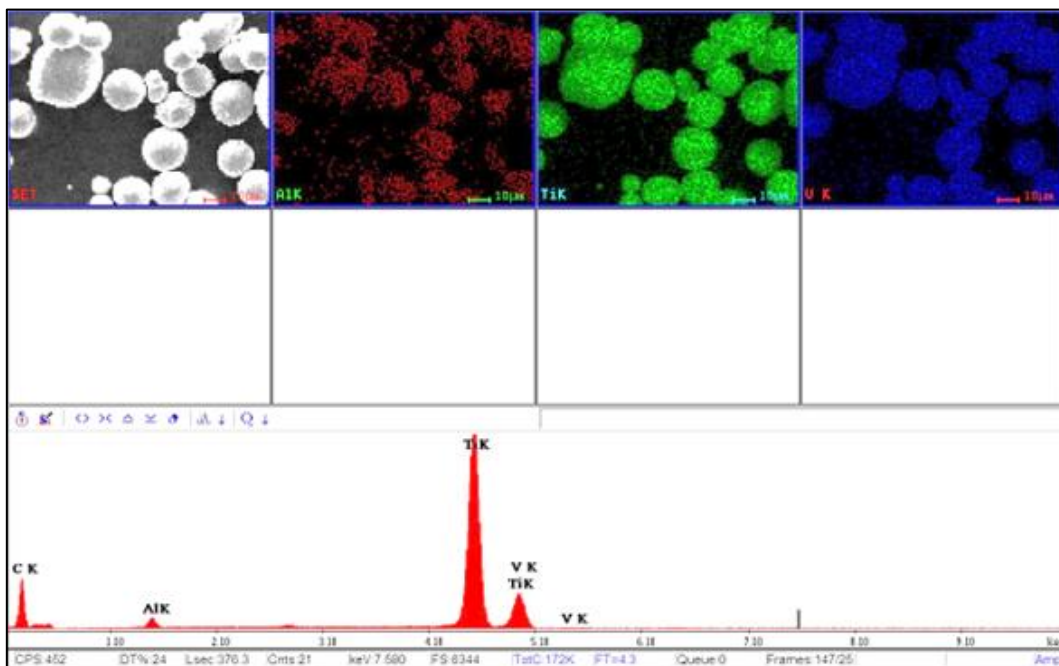


Figure 7. Mapping analysis of Ti-6%Al-4%V

This project has been funded with support from the Erasmus+ Programme Key Action 2 Cooperation Partnerships for Higher Education (KA220-HED). This publication [communication] reflects the views only of the authors, and the Commission cannot be held responsible for any use which may be made of the information contained therein.

In Figure 7, the morphology of the Ti-6%-4%V powder obtained by the hydride-dehydride process (HDH) is presented, which is very fine on the order of microns, and the shape of the grains is approximately spherical, also the homogeneity of the distribution of chemical elements in the structure of the grains can be noted. The In the Mapping analysis of the Ti-6Al-4V can remark the uniformity distribution of the chemical elements Ti, Al, and V, as in Figure 7.

4 Experimental research concerning lattice structures made by Ti6Al4V powders using Selective Laser Melting

In the Figure 8 shows the SEM analysis of the lattice structure, the clearly delimited shape of the 3D printed structure can be noted. Selective laser melting, using high laser powers allows obtaining a structure with fine roughness and complex details, with much better 3D printing performance than in the case of DMLS (direct metal laser sintering). The angle between the rectangular shapes is almost 91.5° , and the wall thickness is around $402.24 - 403.92 \mu\text{m}$, the rectangular shapes dimensions is $909.65 \times 956.17 \mu\text{m}$, as is shown in Figure 8a). In case of SLM technology the precision of the lattice structures is very great of nanometers orders.

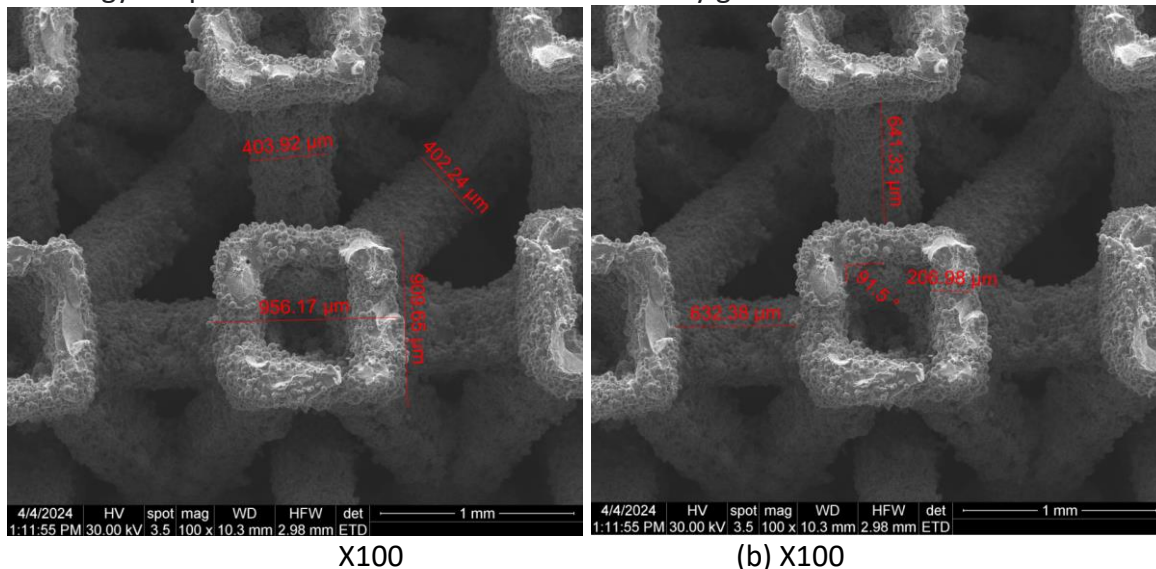
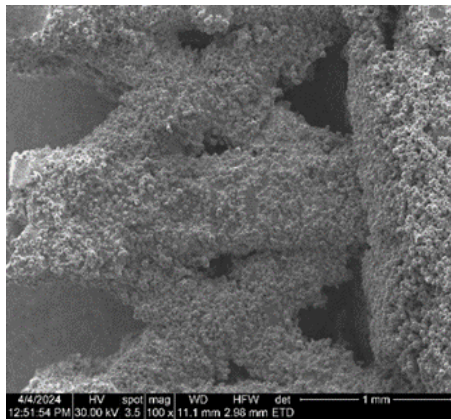
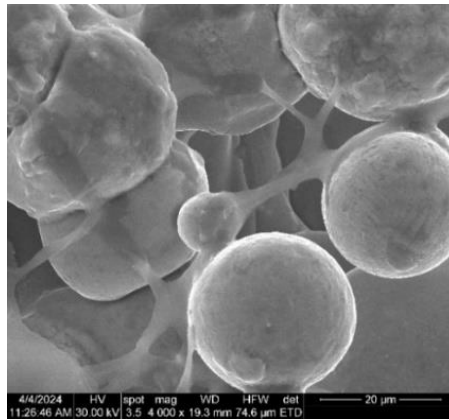


Figure 8. SEM analysis on surface of lattice structure of Ti6Al4V, manufactured by SLM (X100)

This project has been funded with support from the Erasmus+ Programme Key Action 2 Cooperation Partnerships for Higher Education (KA220-HED). This publication [communication] reflects the views only of the authors, and the Commission cannot be held responsible for any use which may be made of the information contained therein.

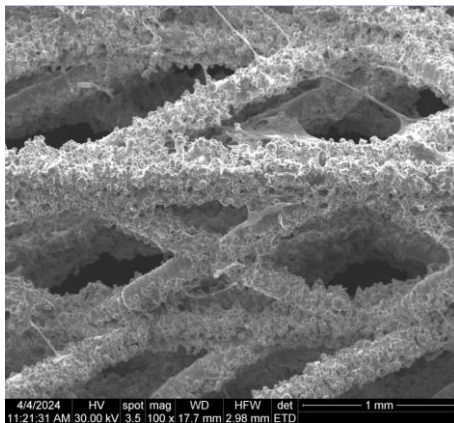


X100

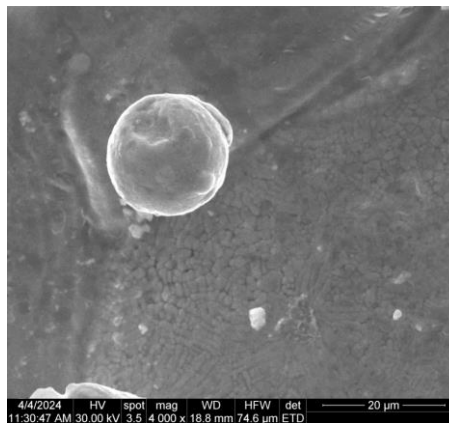


(b) X4000

Figure 9. SEM analysis in section of lattice structure of Ti6Al4V, manufactured by SLM (X100, x4000)



X100



(b) X4000

Fig.10. SEM analysis in section of lattice structure of 625 Inconel, manufactured by SLM (X100, x4000)

Figure 9 shows a lattice structure in section printed by SLM technology and can remark the porosity and the metal bridges that are made between the metal grains, and the great accuracy of 3D printing. The SEM analysis in section presents the fines geometrical details of lattice structure of 625 Inconel sample, manufactured by SLM.

This project has been funded with support from the Erasmus+ Programme Key Action 2 Cooperation Partnerships for Higher Education (KA220-HED). This publication [communication] reflects the views only of the authors, and the Commission cannot be held responsible for any use which may be made of the information contained therein.

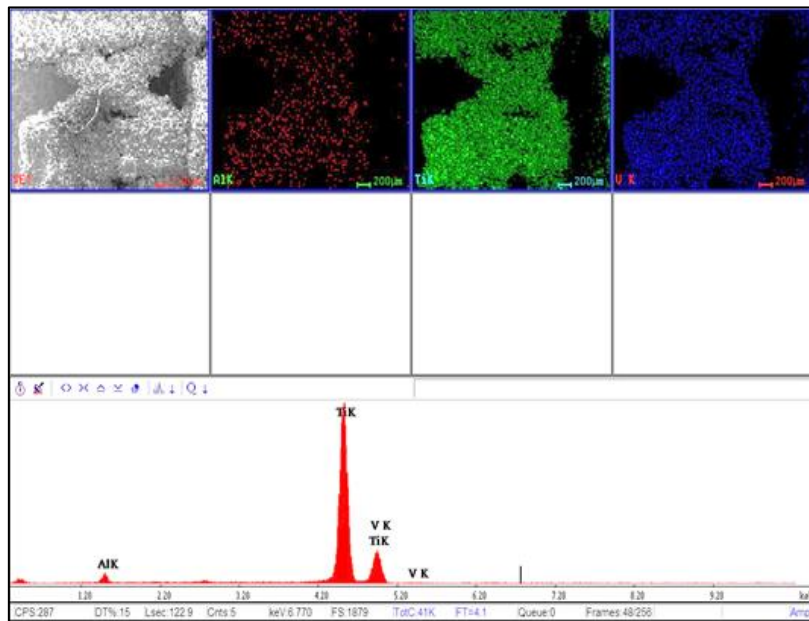


Figure 11. Mapping analysis of Ti-6%Al-4%V

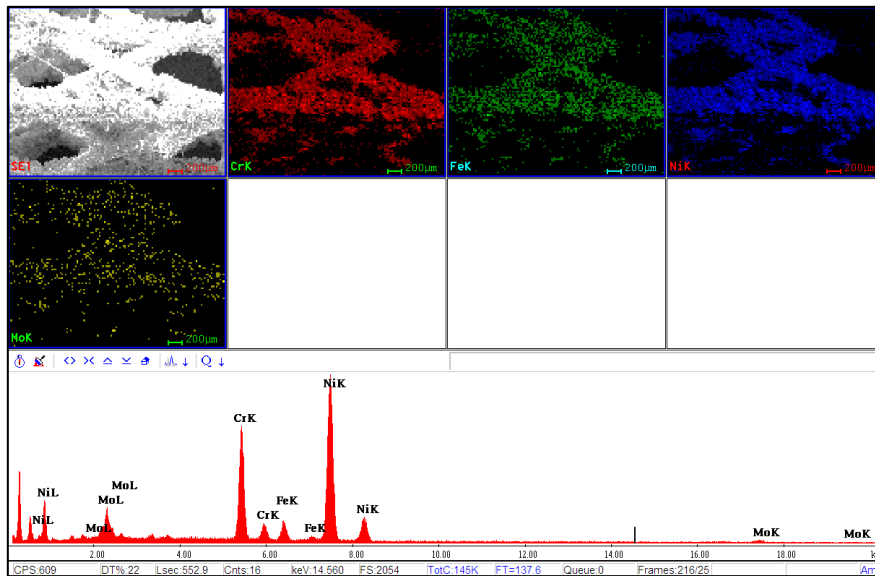


Figure 12. Mapping analysis of 625 Inconel

This project has been funded with support from the Erasmus+ Programme Key Action 2 Cooperation Partnerships for Higher Education (KA220-HED). This publication [communication] reflects the views only of the authors, and the Commission cannot be held responsible for any use which may be made of the information contained therein.

The mapping analysis from Figure 11 shows the chemical composition of the Ti-6%Al-4%V alloy, noting the uniform and homogeneous distribution of the chemical elements (Ti, Al, V) that make up the lattice structure. Concerning the Mapping analysis of 625 Inconel can remark the chemical compound uniform distribution (Cr, Fe, Ni, Mo) on all lattice structure, as in Figure 12.

XRD analysis of Ti6Al4V lattices manufactured by SLM

The XRD analysis of Ti-6%Al-4V lattices manufactured by SLM is presented in Figure 13. Results of the quantitative analysis of the elemental composition by the X-ray fluorescence method (an important note - the object was studied "as is" without its dispersion):

Table 2. Material components correspond to the VT6 or VT6C alloy

Element	Mass fraction, %	VT6 according to GOST 19807–91* 1.14	C VT6 according to GOST 19807–91* 2.11
13 Al	5.194±0.059	5.30-6.50	5.30-6.80
14 Si	0.200±0.010	0.00-0.15	0.00-0.10
22 Ti	90.012±0.076	basis	basis
23 V	4.375±0.053	3.50-4.50	3.50-5.30
26 Fe	0.202±0.007	0.00-0.25	0.00-0.60
28 Ni	0.012±0.002		
42 Mo	0.005±0.001		
undetected elements:			
1 H		0.00-0.02	0.00-0.02
6 C		0.00-0.10	0.00-0.10
7N		0.00-0.10	0.00-0.10
8 O		0.00-0.15	0.00-0.20
24 Ct		0.00-0.08	0.00-0.08
25Mn		0.00-0.07	0.00-0.07
40 Zr		0.00-0.30	0.00-0.30

This project has been funded with support from the Erasmus+ Programme Key Action 2 Cooperation Partnerships for Higher Education (KA220-HED). This publication [communication] reflects the views only of the authors, and the Commission cannot be held responsible for any use which may be made of the information contained therein.

According to GOST 19807–91 (Table 2) the content of the material components corresponds to the VT6 or VT6C alloy. The analogues in USA are Ti-6Al-4V or Ti-Al-V- UNS R56400, TC4, Ti64, ASTM Grade 5.

Table 3. The range of alloying for industrial alloy Ti-6%Al-4%V [25]

Fe	C	Si	V	N	Ti	Al	Zr	O	H	impurities
< 0.6	< 0.1	< 0.1	3.5 - 5.3	< 0.05	86.45 - 90.9	5.3 - 6.8	< 0.3	< 0.2	< 0.015	0.3

In general, the obtained results regarding the content of alloying elements in the titanium matrix differ slightly from the range of alloying/doping with aluminum and vanadium for the industrial alloy Ti-6Al-4V (Table 3, [25])

Table 4. Minimum and maximum content for Ti-6%Al-4%V

Element	Content (wt %)	
	Minimum	Maximum
Al	6.12	6.15
V	3.90	4.00
Fe	0.17	0.18
N	0.01	0.01
C	0.03	0.03
O	0.11	0.12
H	0.004	0.005
Y	0.0020	0.0021
Ti	Balance	

The differences can be explained by the fact that the results were obtained by studying only the near-surface area of the material without dispersion or deep cleaning of the surface
The results of the structural analysis of the material (an important note - the object was studied "as is" without its dispersion):

This project has been funded with support from the Erasmus+ Programme Key Action 2 Cooperation Partnerships for Higher Education (KA220-HED). This publication [communication] reflects the views only of the authors, and the Commission cannot be held responsible for any use which may be made of the information contained therein.

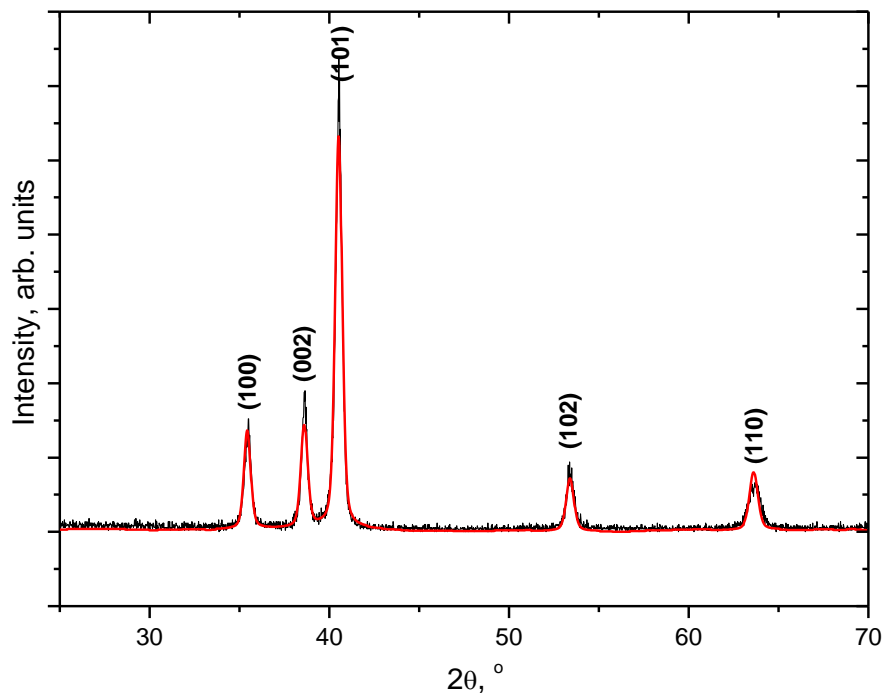


Figure 13. XRD analysis of Ti6Al4V sample manufactured by SLM (Selective Laser Melting)

According to the results of the Rietveld analysis of the diffractogram using the Match!3.0 software package, the sample material is characterized by a close-packed crystalline structure with hexagonal symmetry (space symmetry group is P63/mmc). According to the results of X-ray fluorescence analysis, this structure can be matched to a single-phase alloy based on alpha-titanium (it corresponds to references [27]).

The lattice parameters of the alpha-titanium are $a_0 = 2.95111 \text{ \AA} \pm 6 \cdot 10^{-5}$ and $c_0 = 4.68433 \text{ \AA} \pm 10 \cdot 10^{-5}$, for the studied sample material the lattice parameters are $a_0 = 2.92202 \text{ \AA} \pm 25 \cdot 10^{-5}$ and $c_0 = 4.594233 \text{ \AA} \pm 73 \cdot 10^{-5}$. It is seen a systematic decrease of the lattice parameters of the sample material in comparison to "pure" titanium. It indicates that the sample material is a replacement alloy. According to the X-ray fluorescence spectroscopy data, the sample material was tentatively identified as a titanium alloy Ti-6Al-4V, typically formed by an alpha phase VT6 with a hexagonal crystal structure (P63 / mmc) and a beta phase VT6C with a cubic crystal structure (Im-3m). At the same time, aluminum stabilizes the alpha phase, and vanadium stabilizes the beta phase. The obtained diffractogram does not show reflections

This project has been funded with support from the Erasmus+ Programme Key Action 2 Cooperation Partnerships for Higher Education (KA220-HED). This publication [communication] reflects the views only of the authors, and the Commission cannot be held responsible for any use which may be made of the information contained therein.



corresponding to the cubic volume-centered phase of titanium, but this is a typical situation in X-ray structural studies of Ti-6Al-4V alloys, described, in particular by Fiolek [25]. Lattice parameters for Ti-6Al-4V alloy with different oxygen content are given in table 5 [26]. The values obtained for the researched sample are relatively lower.

Table 5. Lattice parameters for Ti-6Al-4V alloy with different oxygen content

Alloy	<i>a</i> /nm	<i>c</i> /nm	<i>c/a</i>
Ti-6Al-4V-0.17O	0.2944	0.4677	1.58865
Ti-6Al-4V-0.20O	0.2945	0.4679	1.58879
Ti-6Al-4V-0.23O	0.2948	0.4685	1.58921

Even if the content of alloying impurities in the subsurface layers and in the volume is the same within the frames of error (the verification of this assumption requires the destroying of the sample, therefore it is a separate task), the recorded "reduction" of the lattice parameters of the sample material in comparison with the expected values cannot be explained. Probably, the recorded values are the result of physical and (or) physical and chemical effects on the material during sample creation from the powder, which consists on particles of 30-50 microns in size (estimated). According to the analysis by Scherer's method, the size of the regions of coherent scattering for the alpha titanium phase in the sample material is 30-35 nm.

Concerning the research of density by the method of hydrostatic weighing, the studied sample has a density of 4.20(3) g/cm³. A density of 4.45 g /cm³ characterizes the bulk Ti-6Al-4V alloy. Thus, the porosity of the studied sample is about 6%.

9 Conclusions

This research presents the morphology of different metallic powders used in Selective Laser Melting, realizing different Mapping analyses, and establishing the chemical composition. The authors designed various types of lattice structures, from different metallic powders, as Ti-6Al-4V, and Inconel, and examined their detailed morphology and the chemical elements distribution. Selective laser melting (SLM) is used for manufacturing parts, a high-power-density fiber laser (ytterbium fiber laser) to melt and fuse metallic powders to form a 3-dimensional part, being similar to Selective Laser Sintering (SLS). The CAD model of lattice structures is sliced into 2-dimensional layers and transferred to the SLM manufacturing system. Moreover, then, an even layer of powder material is distributed using a roller. The

This project has been funded with support from the Erasmus+ Programme Key Action 2 Cooperation Partnerships for Higher Education (KA220-HED). This publication [communication] reflects the views only of the authors, and the Commission cannot be held responsible for any use which may be made of the information contained therein.



Co-funded by the
Erasmus+ Programme
of the European Union



manufacturing process takes place under a tightly controlled inert atmosphere (argon), the laser then scans and fuses the layer following the geometric information of the sliced model. These scanning/merging and layering processes are repetitive until the final piece is completed. The finished part is removed from the powder bed and undergoes post-processing steps such as heat treatment etc. Lattice structures present fine details of the order of microns, the structure obtained having both homogenous distribution of chemical elements and porosity, its weight being much lower than in the case of cast parts, this being necessary in the case of the medical and aeronautical industries. The morphology structure and XRD analysis were established for the lattice structure of Ti-6Al-4V manufactured by SLM.

In the future, it is desired to continue the development of different types of lattice structures, which are often used in the medical industry, the aeronautical and aerospace industry, for certain structures that must have as little weight as possible.

Morphological SEM analyses were developed, and the chemical composition and the distribution was determined using EDAX analysis for different types of metallic powders from Ti-6%Al-4%V, Inconel 625 and Inconel 718. They were presented SEM, EDAX and Mapping analyses for different metallic powders of Ti-6%Al-4%V, Inconel 625 and Inconel 718 used in Selective Laser Melting process. In this article were designed certain lattice structures with fine details of nanometers order as the wall thickness that it is around 402.24 - 403.92 μm and having great angular precision of 91.5° for Ti-6%Al-4%V and 625 Inconel, manufactured by SLM (Selective Laser Melting). In this paper were determined the SEM and EDAX analysis to establish the morphology structure of lattices structures made by Ti-6%Al-4%V and 625 Inconel, the chemical composition and the uniformity distribution making the Mapping analysis.

Based on the generalization of the results obtained by X-ray fluorescence spectroscopy (Expert 3L spectrometer-analyzer) and X-ray structural analysis (Shimadzu XRD-7000 X-ray diffractometer), it was found that the sample material is an alloy of titanium and aluminum and vanadium of the Ti-6Al-4V alloy type. A comparison of the obtained data allows us to confirm that the sample was produced by the method of layer-by-layer laser melting of Ti-6Al-4V alloy powder with particle sizes of 30-50 microns and a final sample porosity is about 6%. In the aerospace field, there is a decrease in the weight of small parts sizes up to 25-50%, "buy to fly ratio", in the case of using lattice structures and their manufacture by SLM technology. This is very important especially in the field aeronautical, where every kg counts during flight and in terms of kerosene consumption.

This project has been funded with support from the Erasmus+ Programme Key Action 2 Cooperation Partnerships for Higher Education (KA220-HED). This publication [communication] reflects the views only of the authors, and the Commission cannot be held responsible for any use which may be made of the information contained therein.





References

1. Antanasova, M., Kocjan, A., Kovač, J., Žužek, B., Jevnikar, P. (2018). Influence of thermo-mechanical cycling on porcelain bonding to cobalt–chromium and titanium dental alloys fabricated by casting, milling, and selective laser melting. *J. Prosthodont. Res.* 2018, 62, 184–194. <https://doi.org/10.1016/j.jpor.2017.08.007>
2. Baila, D.I., Sanfilippo, F., Savu, T., Górski, F., Radu, I.C., Zaharia, C., Parau, C.A., Zelenay, M. and Razvan, P. (2024), "3D printing of personalised stents using new advanced photopolymerizable resins and Ti-6Al-4V alloy", *Rapid Prototyping Journal*, Vol. 30 No. 4, pp. 696-710. <https://doi.org/10.1108/RPJ-10-2023-0360>
3. Balbaa, M., Mekhiel, S., Elbestawi, M. McIsaac, J. On selective laser melting of Inconel 718: Densification, surface roughness, and residual stresses, *Materials & Design*, Volume 193, 2020, 108818, <https://doi.org/10.1016/j.matdes.2020.108818>.
4. Băilă, D.-I.; Păcurar, R.; Savu, T.; Zaharia, C.; Truşcă, R.; Nemeş, O.; Górski, F.; Păcurar, A.; Pleşa, A.; Sabău, E. Mechanical and Wetting Properties of Ta₂O₅ and ZnO Coatings on Alloy Substrate of Cardiovascular Stents Manufactured by Casting and DMLS. *Materials* **2022**, *15*, 5580. <https://doi.org/10.3390/ma15165580>
5. Băilă, D.-I.; Vițelaru, C.; Truşcă, R.; Constantin, L.R.; Păcurar, A.; Parau, C.A.; Păcurar, R. Thin Films Deposition of Ta₂O₅ and ZnO by E-Gun Technology on Co-Cr Alloy Manufactured by Direct Metal Laser Sintering. *Materials* **2021**, *14*, 3666. <https://doi.org/10.3390/ma14133666>
6. Beshchasna, N., Saqib, M., Kraskiewicz, H., Wasyluk, Ł., Kuzmin, O., Duta, O.C., Ficai, D., Ghizdavet, Z., Marin, A., Ficai, A. (2020). Recent Advances in Manufacturing Innovative Stents. *Pharmaceutics*, 12, 349. <https://doi.org/10.3390/pharmaceutics12040349>
7. Borhani, S., Hassanajili, S., Tafti, S.H.A., Rabbani, S. (2018). Cardiovascular stents: Overview, evolution, and next generation. *Prog. Biomater.*, 7, 175–205. <https://doi.org/10.1007/s40204-018-0097-y>
8. Brambilla, A., Pennati, G., Petrini, L., Berti, F. (2023). Stents in Congenital Heart Disease: State of the Art and Future Scenarios. *Appl. Sci.*, 13, 9692. <https://doi.org/10.3390/app13179692>
9. Caracciolo, A., Mazzone, P., Lattera, G., Garcia-Ruiz, V., Polimeni, A., Galasso, S., Saporito, F., Carerj, S., D'Ascenzo, F., Marquis-Gravel, G., (2019). Antithrombotic Therapy for Percutaneous Cardiovascular Interventions: From Coronary Artery Disease to Structural Heart Interventions. *J. Clin. Med.*, 8, 2016. <https://doi.org/10.3390/jcm8112016>
10. Černov, N. (2011). Circular and linear regression: fitting circles and lines by least squares. Boca Raton, Fla. London: CRC.
11. Dahiya, U.R., Singh, S., Garg, C.K, Rai, A., Kalyanasundaram, D (2022). Modified Surface Composition and Biocompatibility of Core-Shell Nitinol Nanoparticles Fabricated via Laser Ablation of Differently Passivized Targets. *Front. Mater.* 9:855705. <https://doi.org/10.3389/fmats.2022.855705>
12. Fu, W., Liu, S., Jiao, J., Xie, Z., Huang, X., Lu, Y., Liu, H., Hu, S., Zuo, E., Kou, N.; (2022). Wear Resistance and Biocompatibility of Co-Cr Dental Alloys Fabricated with CAST and SLM Techniques. *Materials*, 15, 3263. <https://doi.org/10.3390/ma15093263>
13. Gerontas, A., Avgerinos, D., Charitakis, K., Maragou, H, Drosatos, K., (2023). Contributions of physicians and researchers of Greek descent in the advancement of clinical and experimental cardiology and cardiac surgery. *Front. Cardiovasc. Med.* 10: 1231762. <https://doi.org/10.3389/fcvm.2023.1231762>
14. Guerra, J. A, Ciurana, J. (2019). Stent's Manufacturing Field: Past, Present, and Future Prospects. *Angiography. IntechOpen.* <https://doi.org/10.5772/intechopen.81668>
15. Hoare, D., Bussooa, A., Neale, S., Mirzai, N., Mercer, J. (2019). The future of cardiovascular stents: Bioresorbable and integrated biosensor technology. *Adv. Sci.*, 6, 1900856. <https://doi.org/10.1002/advs.201900856>

This project has been funded with support from the Erasmus+ Programme Key Action 2 Cooperation Partnerships for Higher Education (KA220-HED). This publication [communication] reflects the views only of the authors, and the Commission cannot be held responsible for any use which may be made of the information contained therein.



16. Kan, X., Ma, T., Dong, Z., Xu, X.Y. (2021). Patient-Specific Virtual Stent-Graft Deployment for Type B Aortic Dissection: A Pilot Study of the Impact of Stent-Graft Length, *Front. Physiol.*, 26 July 2021, Sec. Computational Physiology and Medicine, 12, <https://doi.org/10.3389/fphys.2021.718140>
17. Leary, M., Mazur, M., Williams, H., Yang, E., Alghamdi, A., Lozanovski, B., Zhang, X., Shidid, D., Farahbod-Sternahl, L., Witt, G., Kelbassa, I., Choong, P., Qian, M., Brandt, M. Inconel 625 lattice structures manufactured by selective laser melting (SLM): Mechanical properties, deformation and failure modes, *Materials & Design*, Volume 157, 2018, Pages 179-199, <https://doi.org/10.1016/j.matdes.2018.06.010>
18. Lin, L.-H., Ho, K.-L., Jian, Y.-M., Chiang, K.-H., Hsiao, H.-M. (2023). Effects of Tapered-Strut Design on Fatigue Life Enhancement of Peripheral Stents. *Bioengineering*, 10, 443. <https://doi.org/10.3390/bioengineering10040443>
19. Málaga-Chuquitaype, C. (2022). Machine Learning in Structural Design: An Opinionated Review. *Front. Built Environ.* 8:815717. <https://doi.org/10.3389/fbuil.2022.815717>
20. McGee, O.M., Geraghty, S., Hughes, C., Jamshidi, P., Kenny, D. P., Attallah, M.M., Lally, C. (2022). An investigation into patient-specific 3D printed titanium stents and the use of etching to overcome Selective Laser Melting design constraints, *Journal of the Mechanical Behavior of Biomedical Materials*, 134, 105388, <https://doi.org/10.1016/j.jmbbm.2022.105388>
21. Păcurar RI, Sanfilippo F, Økter MB, Băilă D-I, Zaharia C, Nicoară AI, Radu IC, Savu T, Górski F, Kuczko W, Wichniarek R, Comşa DS, Zelenay M and Woźniak P (2024) Use of high-performance polymeric materials in customized low-cost robotic grippers for biomechatronic applications: experimental and analytical research. *Front. Mater.* 11:1304339. doi: 10.3389/fmats.2024.1304339
22. Peng, X., Kong, L., Fuh, J.Y.H., Wang, H. (2021). A Review of Post-Processing Technologies in Additive Manufacturing. *J. Manuf. Mater. Process.*, 5, 38. <https://doi.org/10.3390/jmmp5020038>
23. Revilla-León, M., Meyer, M.J., Özcan, M. (2019). Metal additive manufacturing technologies: Literature review of current status and prosthodontic applications. *Int. J. Comput. Dent.*, 22, 55–67. PMID: 30848255.
24. Wu, S., Zeng, J., Li, H., Han, C., Wu, W., Zeng, W., Tang, L. (2023). A Review on the Full Chain Application of 3D Printing Technology in Precision Medicine. *Processes*, 11, 1736. <https://doi.org/10.3390/pr11061736>
25. Fiolek, A.; Zimowski, S.; Kopia, A.; Moskalewicz, T. The Influence of Electrophoretic Deposition Parameters and Heat Treatment on the Microstructure and Tribological Properties of Nanocomposite Si₃N₄/PEEK 708 Coatings on Titanium Alloy. *Coatings* 2019, 9, 530. <https://doi.org/10.3390/coatings9090530>
26. Tang, L.; Fan, J.; Kou, H.; Tang, B.; Li, J. Effect of Oxygen Variation on High Cycle Fatigue Behavior of Ti-6Al-4V Titanium Alloy. *Materials* 2020, 13, 3858. <https://doi.org/10.3390/ma13173858>
27. Wood, R.M., The lattice constants of high purity alpha titanium, *Proceedings of the physical Society*, vol.80, nb.3, 1962 *Proc.Phys. Soc.* 80 783, DOI 10.1088/0370-1328/80/3/323
28. <https://en.wikipedia.org/wiki/Inconel>

This project has been funded with support from the Erasmus+ Programme Key Action 2 Cooperation Partnerships for Higher Education (KA220-HED). This publication [communication] reflects the views only of the authors, and the Commission cannot be held responsible for any use which may be made of the information contained therein.



Co-funded by the
Erasmus+ Programme
of the European Union



Erasmus+ Programme Key Action 2 Cooperation Partnerships for Higher Education
(KA220-HED)

Project No: 2023-1-RO01-KA220-HED-000155412

Project title: European Network for Additive Manufacturing in Industrial Design for
Ukrainian Context – Acronym: AMAZE

IO3 – AMAZE VR/AR e-learning platform for virtual laboratory

Project Title	European Network for Additive Manufacturing in Industrial Design for Ukrainian Context 2023-1-RO01-KA220-HED-000155412
Output	IO3 - AMAZE VR/AR e-learning platform for virtual laboratory used for Additive Manufacturing of industrial parts
Date of Delivery	September 2024
Location	EDIBON International S.A., Spain
Version	FINAL VARIANT, *14.09.2024

This project has been funded with support from the Erasmus+ Programme Key Action 2 Cooperation Partnerships for Higher Education (KA220-HED). This publication [communication] reflects the views only of the authors, and the Commission cannot be held responsible for any use which may be made of the information contained therein.





Co-funded by the
Erasmus+ Programme
of the European Union



1 Introduction in Augmented Reality

Definition: Augmented Reality (AR) is a technology that overlays digital information onto the real world. (Fig. 1)



Fig.1. Virtual reality

Difference between AR and VR:

AR enhances the real world, while Virtual Reality (VR) creates a completely virtual environment. (Fig. 2)



Fig.2. AR smart glasses

This project has been funded with support from the Erasmus+ Programme Key Action 2 Cooperation Partnerships for Higher Education (KA220-HED). This publication [communication] reflects the views only of the authors, and the Commission cannot be held responsible for any use which may be made of the information contained therein.



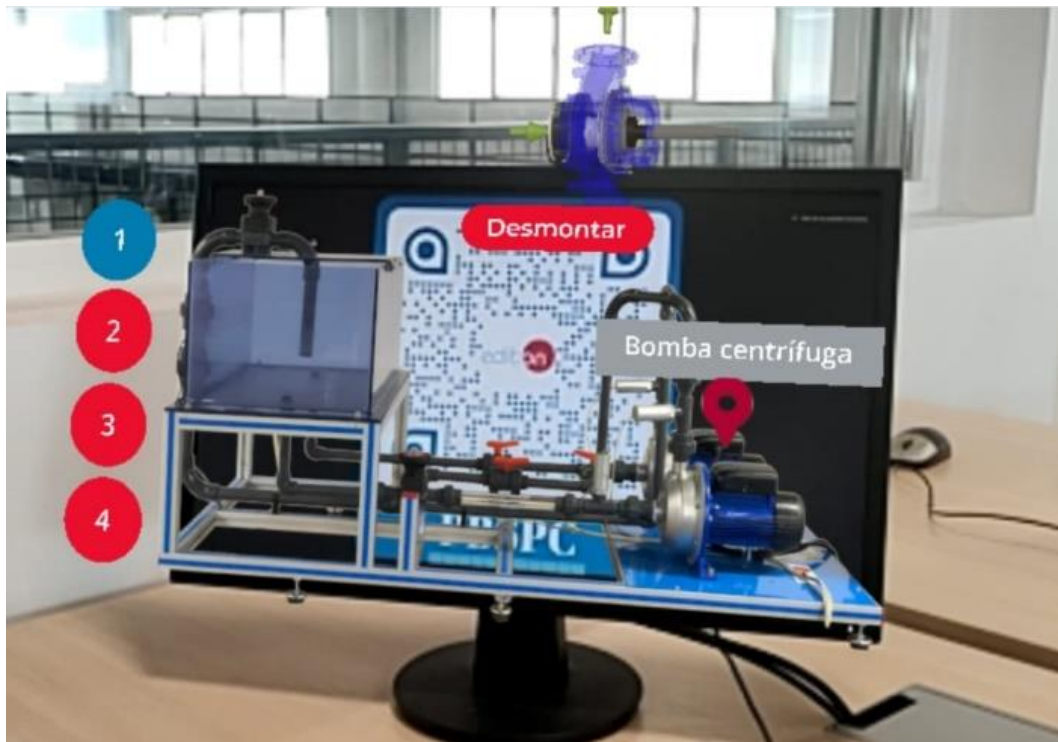


Fig.3. Augmented Reality

How Augmented Reality Works (Fig. 3)

Essential Components:

- Hardware: Cameras (capture real-world), sensors (position and orientation), displays (present the augmented view)
- Software: Computer vision (processes and interprets real-world), Simultaneous Localization and Mapping – SLAM (algorithms for environment and position), Rendering Engine (generating digital content)
- Process: Capturing the real world, processing digital overlays, and displaying the combined view to the user.

This project has been funded with support from the Erasmus+ Programme Key Action 2 Cooperation Partnerships for Higher Education (KA220-HED). This publication [communication] reflects the views only of the authors, and the Commission cannot be held responsible for any use which may be made of the information contained therein.



Fig.4. VR/AR applications in industry

Applications in Industry: (Fig.4)

Healthcare: Surgery assistance, medical training (Fig.5)

Education: Interactive learning, virtual classrooms (Fig.6)

Entertainment: Gaming, immersive experiences (Fig.7)

Retail: Virtual try-ons, enhanced shopping experiences (Fig.8)

Tourism: Interactive tours, historical reconstructions (Fig.9)

Industry: manufacture, design (Fig.10)

This project has been funded with support from the Erasmus+ Programme Key Action 2 Cooperation Partnerships for Higher Education (KA220-HED). This publication [communication] reflects the views only of the authors, and the Commission cannot be held responsible for any use which may be made of the information contained therein.



Co-funded by the Erasmus+ Programme of the European Union



Fig.5. VR/AR applications in Healthcare



Fig.6. VR/AR applications in Education

This project has been funded with support from the Erasmus+ Programme Key Action 2 Cooperation Partnerships for Higher Education (KA220-HED). This publication [communication] reflects the views only of the authors, and the Commission cannot be held responsible for any use which may be made of the information contained therein.





Fig.7. VR/AR applications in Entertainment



Fig.8. VR/AR applications in Retail

This project has been funded with support from the Erasmus+ Programme Key Action 2 Cooperation Partnerships for Higher Education (KA220-HED). This publication [communication] reflects the views only of the authors, and the Commission cannot be held responsible for any use which may be made of the information contained therein.



Co-funded by the Erasmus+ Programme of the European Union



Fig.9. VR/AR applications in Tourism



Fig.10. VR/AR applications in Industry

This project has been funded with support from the Erasmus+ Programme Key Action 2 Cooperation Partnerships for Higher Education (KA220-HED). This publication [communication] reflects the views only of the authors, and the Commission cannot be held responsible for any use which may be made of the information contained therein.





Co-funded by the
Erasmus+ Programme
of the European Union



Benefits of Augmented Reality (Fig.11 and Fig.12)

Enhanced User Experience: More engaging and interactive

Increased Efficiency: Improved task performance and productivity

Facilitates Learning and Training: Hands-on practice in a safe environment

Challenges and Limitations

Technical Issues: Accuracy, latency

Development and Implementation Costs: High initial investment

Ethical and Privacy Concerns: Data security, user consent

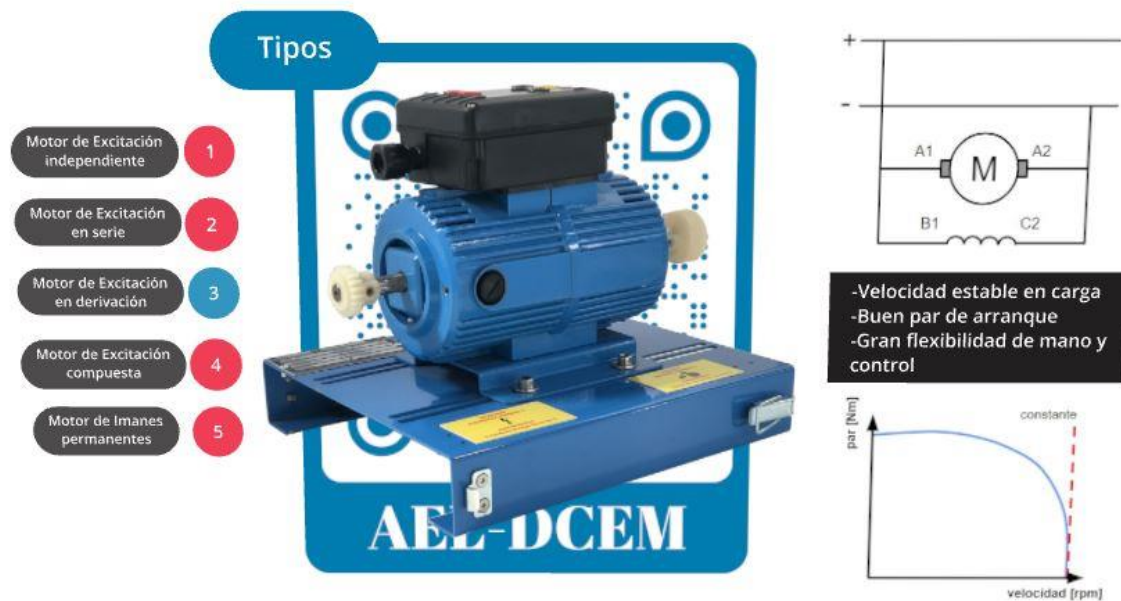


Fig.11.Motor AEL-DCEM

This project has been funded with support from the Erasmus+ Programme Key Action 2 Cooperation Partnerships for Higher Education (KA220-HED). This publication [communication] reflects the views only of the authors, and the Commission cannot be held responsible for any use which may be made of the information contained therein.





Co-funded by the
Erasmus+ Programme
of the European Union

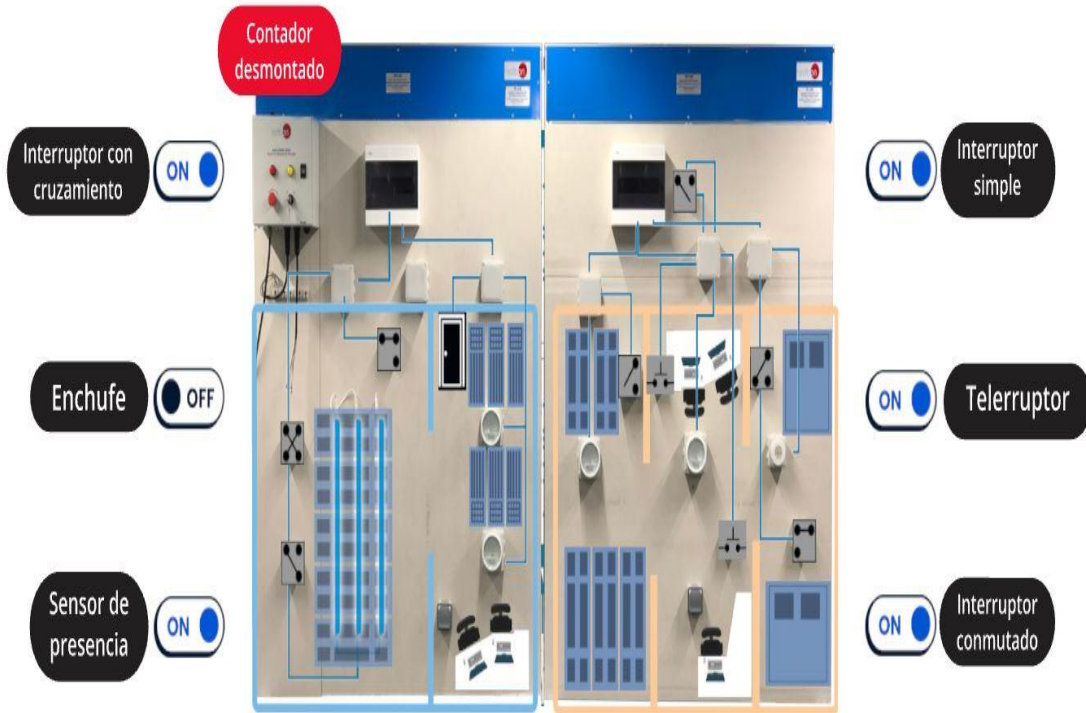


Fig.12. Disassembled counter

Future of Augmented Reality

Emerging Trends: More integrated AR experiences, wearable AR devices

Technological Innovations: Improved hardware, AI integration

Potential Impact: Greater societal adoption, new business models, as in Fig.13.

This project has been funded with support from the Erasmus+ Programme Key Action 2 Cooperation Partnerships for Higher Education (KA220-HED). This publication [communication] reflects the views only of the authors, and the Commission cannot be held responsible for any use which may be made of the information contained therein.





Co-funded by the Erasmus+ Programme of the European Union

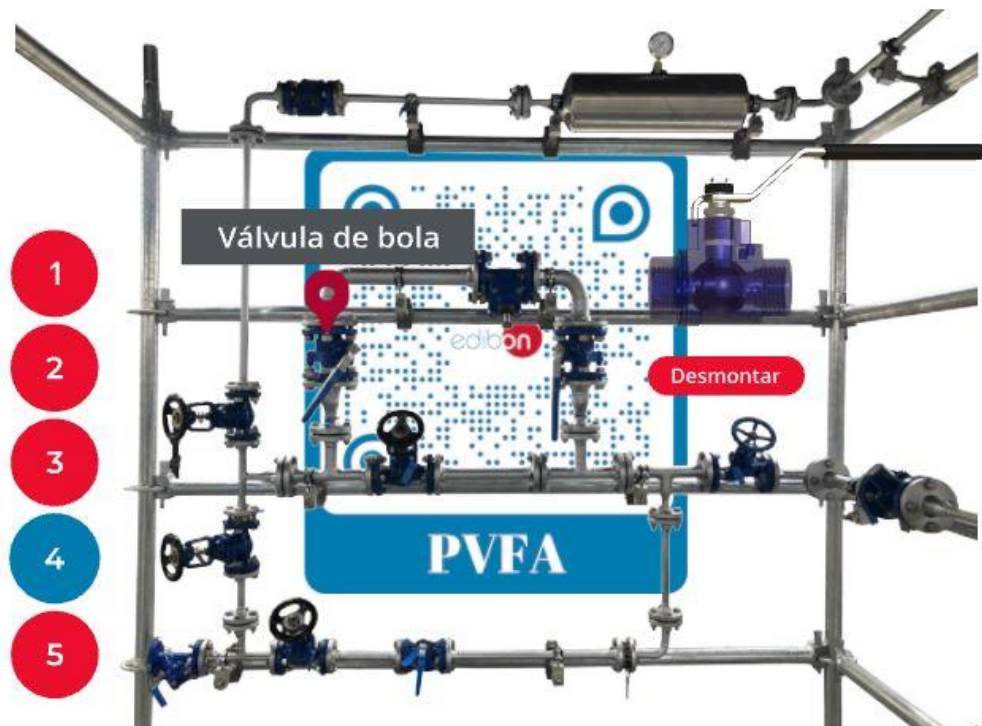


Fig.13. Ball valve

Conclusions

The VR/AR platform represents a significant advancement in the field of distance learning, specifically designed for additive manufacturing. This innovative approach seamlessly combines theoretical content with remote practice, offering students a comprehensive and deeply enriching educational experience, as in Fig.14.

This project has been funded with support from the Erasmus+ Programme Key Action 2 Cooperation Partnerships for Higher Education (KA220-HED). This publication [communication] reflects the views only of the authors, and the Commission cannot be held responsible for any use which may be made of the information contained therein.



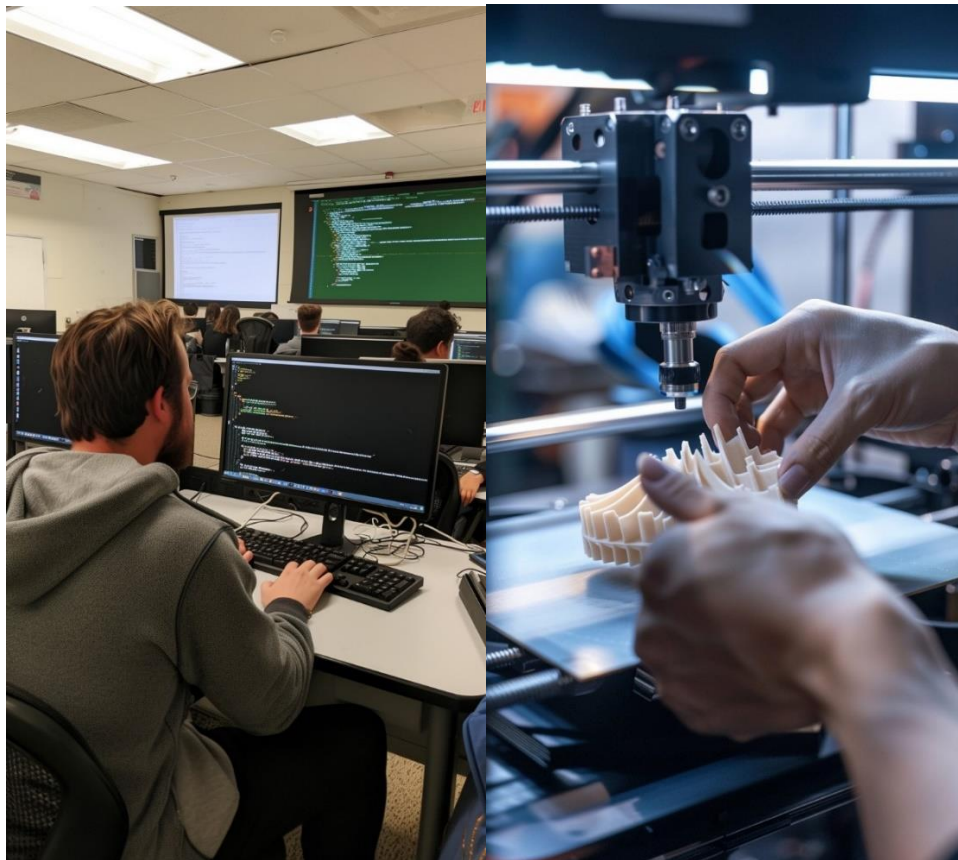


Fig.14. VR/AR e-learning platform used for Additive Manufacturing

In a world where technology evolves at a rapid pace, the ability to adapt to new tools and methodologies is essential. This platform not only provides fundamental theoretical knowledge but also allows students to apply these concepts in a practical environment, even when they are miles away from traditional equipment and laboratories. This unique combination ensures that students not only understand the theoretical principles of additive manufacturing but also develop the practical skills necessary to face the real challenges they will encounter in the industry, especially in Industry 5.0, as in Figure 15.

This project has been funded with support from the Erasmus+ Programme Key Action 2 Cooperation Partnerships for Higher Education (KA220-HED). This publication [communication] reflects the views only of the authors, and the Commission cannot be held responsible for any use which may be made of the information contained therein.

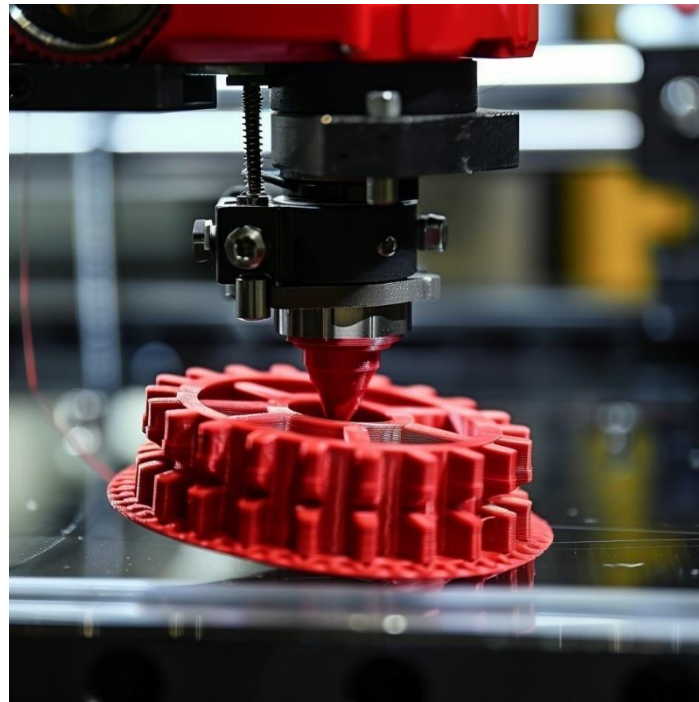


Fig.15. VR/AR e-learning platform combines theoretical principles of additive manufacturing and practical skills for Industry 5.0.

Moreover, the system has been designed to be highly interactive and adaptable to the individual needs of each student. It utilizes advanced simulations and real-time collaboration tools that allow students to experiment and solve problems in a controlled yet dynamic environment. This approach not only enhances knowledge retention but also fosters creativity and critical thinking, qualities that are indispensable in the field of additive manufacturing.

Another key aspect of this platform is accessibility. It is understood that access to specialized equipment can be limited, especially for those living in remote areas or lacking the resources to attend in-person courses. Therefore, an infrastructure has been developed that allows students to interact with state-of-the-art machinery and software from the comfort of their homes. This flexibility not only democratizes access to quality education but also

This project has been funded with support from the Erasmus+ Programme Key Action 2 Cooperation Partnerships for Higher Education (KA220-HED). This publication [communication] reflects the views only of the authors, and the Commission cannot be held responsible for any use which may be made of the information contained therein.



Co-funded by the
Erasmus+ Programme
of the European Union



prepares a new generation of professionals capable of leading the future of digital manufacturing, as in Figure 16.



Fig.16. Accessibility of VR/AR e-learning platform as an educational resource

In summary, this platform is more than just an educational resource; it is a transformative tool that empowers students to face real-world challenges in additive manufacturing. By integrating theoretical knowledge with remote practice, it creates a learning environment that is both accessible and highly effective, preparing students to excel in an ever-evolving industry.

This project has been funded with support from the Erasmus+ Programme Key Action 2 Cooperation Partnerships for Higher Education (KA220-HED). This publication [communication] reflects the views only of the authors, and the Commission cannot be held responsible for any use which may be made of the information contained therein.





Co-funded by the
Erasmus+ Programme
of the European Union



2 References

Books and Publications:

- "The SAGE Handbook of E-learning Research" by Richard Andrews and Caroline Haythornthwaite: a comprehensive resource on e-learning research.
- "Additive Manufacturing Technologies: 3D Printing, Rapid Prototyping, and Direct Digital Manufacturing" by Ian Gibson, David W. Rosen, and Brent Stucker: a key book on additive manufacturing technologies.
- "Teaching in a Digital Age: Guidelines for Designing Teaching and Learning" by A.W. (Tony) Bates: a resource for designing and implementing online courses.

Academic Articles:

- A systematic review on the role of e-learning and virtual laboratories in engineering education. (Educational Research Review)
- "Remote Control of Additive Manufacturing Machines: Enhancing Learning Through Practical Engagement at a Distance" (Journal of Manufacturing Processes).

Articles and Technical Reports:

- "Advances in Remote Monitoring and Control Systems for Manufacturing" (Journal of Manufacturing Systems)
- "The Impact of Distance Learning Technologies on Technical Education in the Manufacturing Industry" (Industry Report, 2023).

This project has been funded with support from the Erasmus+ Programme Key Action 2 Cooperation Partnerships for Higher Education (KA220-HED). This publication [communication] reflects the views only of the authors, and the Commission cannot be held responsible for any use which may be made of the information contained therein.





Co-funded by the
Erasmus+ Programme
of the European Union



Erasmus+ Programme Key Action 2 Cooperation Partnerships for Higher Education
(KA220-HED)

Project No: 2023-1-RO01-KA220-HED-000155412

Project title: European Network for Additive Manufacturing in Industrial Design for
Ukrainian Context – Acronym: AMAZE

IO3 – AMAZE VR/AR e-learning platform for virtual laboratory

Project Title	European Network for Additive Manufacturing in Industrial Design for Ukrainian Context 2023-1-RO01-KA220-HED-000155412
Output	IO3 – AMAZE VR/AR e-learning platform for virtual laboratory
Module	Reverse Engineering
Date of Delivery	September 2024
	Poznań University of Technology, Poland
Version	FINAL VARIANT, *14.09.2024

This project has been funded with support from the Erasmus+ Programme Key Action 2 Cooperation Partnerships for Higher Education (KA220-HED). This publication [communication] reflects the views only of the authors, and the Commission cannot be held responsible for any use which may be made of the information contained therein.





Co-funded by the
Erasmus+ Programme
of the European Union



1. Introduction

Reverse engineering in the context of product manufacturing involves analyzing an existing product to understand its design, functionality, and components. This process can provide valuable insights for various applications in product development and manufacturing. In the toolkit a detailed description of how reverse engineering applies to product manufacturing was presented,

- a) Product Analysis and Improvement
- b) Cost Reduction
- c) Intellectual Property and Innovation
- d) Legacy Products and Support
- e) Quality Control and Testing
- f) Sustainability and Recycling
- g) Rapid Prototyping

Reverse engineering in product manufacturing involves analyzing a product to understand its design, architecture, and functionality. It allows manufacturers to recreate and improve existing products, ensure compatibility, or develop new products based on existing ones. Here are several common techniques used in reverse engineering, which was also detailed described in toolkit:

- Physical Disassembly,
- 3D Scanning,
- Computer-Aided Design (CAD) Reconstruction,
- Material Analysis,
- Functional Analysis,
- Electrical Analysis,
- Software Analysis,
- Prototyping,
- Metrology.

This project has been funded with support from the Erasmus+ Programme Key Action 2 Cooperation Partnerships for Higher Education (KA220-HED). This publication [communication] reflects the views only of the authors, and the Commission cannot be held responsible for any use which may be made of the information contained therein.





Each technique can be utilized individually or in combination, depending on the complexity of the product and the objectives of the reverse engineering process. Reverse engineering plays a crucial role in product development, competitive analysis, and innovation within manufacturing industries, as in Fig.1..

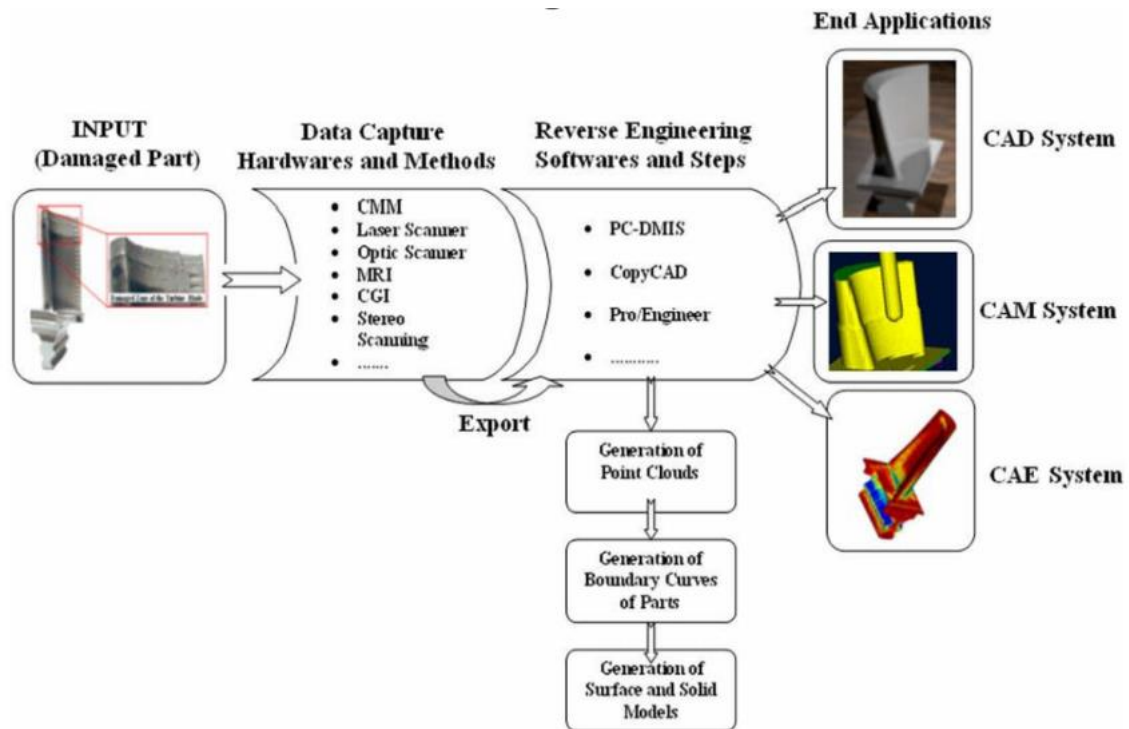


Fig.1. The whole process of RE should be computer-aided

2. Reverse Engineering techniques

2.1 CMM Scanning

CMM scanning is a critical technique used in reverse engineering to create digital representations of physical objects.

This project has been funded with support from the Erasmus+ Programme Key Action 2 Cooperation Partnerships for Higher Education (KA220-HED). This publication [communication] reflects the views only of the authors, and the Commission cannot be held responsible for any use which may be made of the information contained therein.



This process typically involves using advanced imaging technology to capture the geometry, shape, and sometimes even the colour or texture of an object, as in Fig.2.

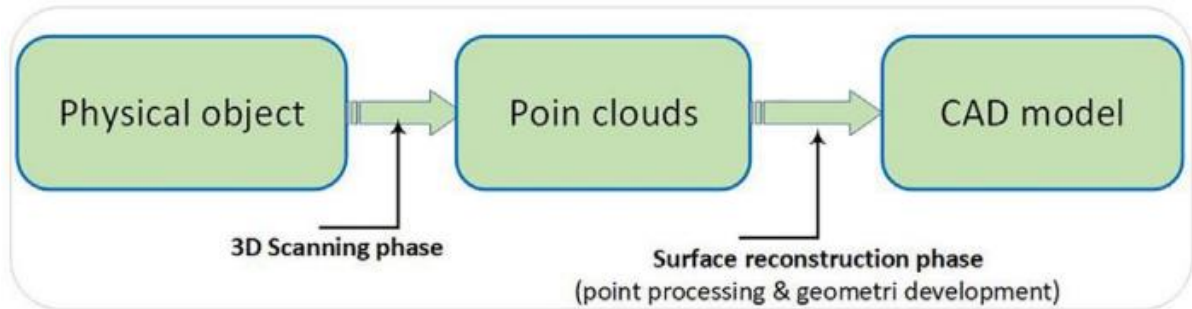


Fig.2. Generic RE process using 3D scanning technology

2.2 Optical Scanning

The purpose of reverse engineering is to manufacture another object based on a physic and existing object for which 3D CAD is not available.

The scanner can convert the physical object into a point cloud. This kind of reverse engineering can be used to make digital 3D record of the objects, for security copies, shows it in presentations to the competitors about how it works, identify potential patent infringement.

3. Application of reverse engineering to the production of biomedical engineering products

Reverse engineering is pivotal in medical life sciences, providing significant advantages such as reduced time and costs, along with enhanced product accuracy. Modern medical production systems integrate advanced measurement techniques to precisely capture human anatomy, sophisticated software for CAD model design, cutting-edge fabrication technologies, and innovative materials for improved manufacturing outcomes. In fields like orthopaedics,

This project has been funded with support from the Erasmus+ Programme Key Action 2 Cooperation Partnerships for Higher Education (KA220-HED). This publication [communication] reflects the views only of the authors, and the Commission cannot be held responsible for any use which may be made of the information contained therein.



dentistry, and reconstructive surgery, reverse engineering enables detailed imaging, modeling, and replication of a patient's bone structure, allowing surgeons to meticulously plan and evaluate procedures before actual implementation.

3.1 Reverse engineering in prosthetic application

Filip Górski and colleagues, in their article "Development and Testing of an Individualized Sensorized 3D Printed Upper Limb Bicycle Prosthesis for Adult Patients" present the design and evaluation of a personalized prosthetic device tailored for an adult patient, specifically for activities such as bicycle riding. The prosthesis was developed using 3D scanning, semi-automated design with the AutoMedPrint system, and low-cost Fused Deposition Modelling (FDM) technology for 3D printing. It features integrated force and movement sensors and was subjected to rigorous testing across various dynamic scenarios to assess functionality, mitigate potential risks, and refine the design prior to activating the end effector. The article comprehensively details the design, production, and testing processes, showcasing the successful implementation and identifying areas for mechanical and electrical improvements, as in Figures 3 and 4.

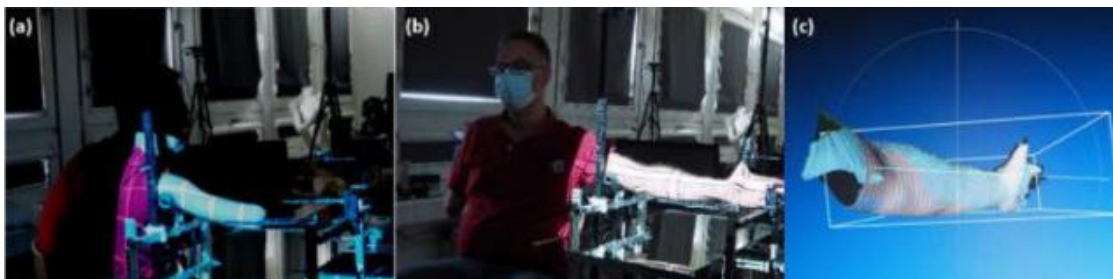


Fig.3. 3D scanning of patient, (a) stump; (b) healthy arm; and (c) mesh data during processing

This project has been funded with support from the Erasmus+ Programme Key Action 2 Cooperation Partnerships for Higher Education (KA220-HED). This publication [communication] reflects the views only of the authors, and the Commission cannot be held responsible for any use which may be made of the information contained therein.



Fig.4. Tests of initial, mechanical version of the prosthesis,
(a) laboratory tests and (b) usability tests

3.2 Reverse engineering in hand therapy

The paper "Development and Studies of VR-Assisted Hand Therapy Using a Customized Biomechatronic 3D-Printed Orthosis" authored by Filip Górski and colleagues, explores the creation, testing, and use of a wrist–hand orthosis for hand therapy in a teenage patient with congenital paresis. The team enhanced a standard 3D-printed orthosis with sensors, transforming it into a motion controller for virtual reality (VR). Due to the patient’s wrist and hand impairments, standard VR controllers were not an option, so the orthosis was adapted by integrating custom electronics and motion trackers. A VR game, developed in collaboration with physiotherapists, replaced traditional VR inputs with those from the customized orthosis. This game was then tested on patients and evaluated by an expert to

This project has been funded with support from the Erasmus+ Programme Key Action 2 Cooperation Partnerships for Higher Education (KA220-HED). This publication [communication] reflects the views only of the authors, and the Commission cannot be held responsible for any use which may be made of the information contained therein.



Co-funded by the
Erasmus+ Programme
of the European Union



determine its effectiveness and identify areas for further improvement in the orthosis design.

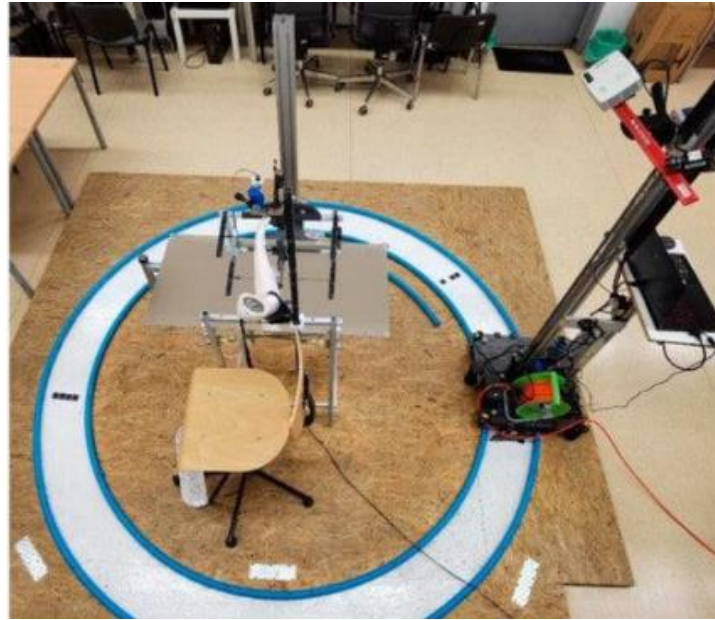


Fig.5. Prototype of AutoMedPrint system (scanning rig)

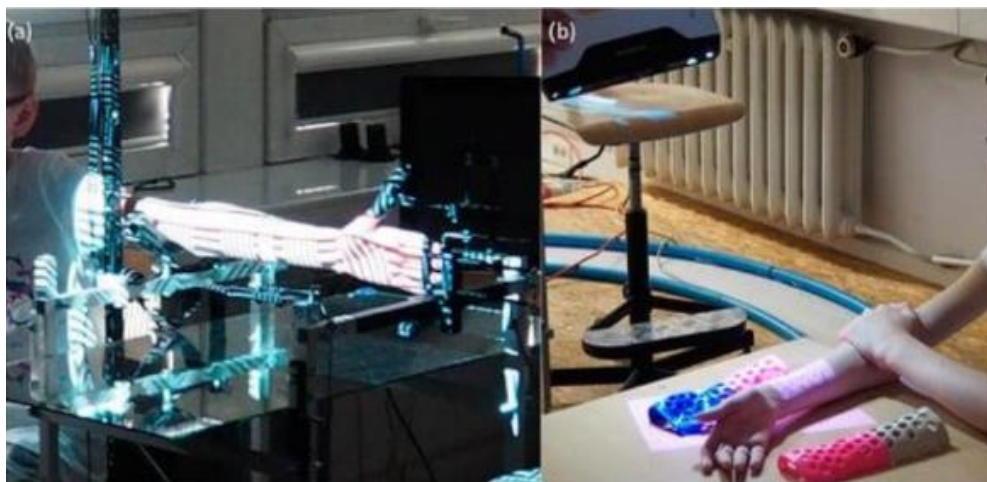


Fig.6. Scanning of the patient, (a) left arm—mechanized rig, (b) right arm—manual scan

This project has been funded with support from the Erasmus+ Programme Key Action 2 Cooperation Partnerships for Higher Education (KA220-HED). This publication [communication] reflects the views only of the authors, and the Commission cannot be held responsible for any use which may be made of the information contained therein.





Fig.7. Customized therapeutic orthosis design and production for the purpose of VR system prototyping



Fig.8. Customized therapeutic orthosis, (a) first version, and (b) second version (10 months later)

This project has been funded with support from the Erasmus+ Programme Key Action 2 Cooperation Partnerships for Higher Education (KA220-HED). This publication [communication] reflects the views only of the authors, and the Commission cannot be held responsible for any use which may be made of the information contained therein.



Smart (Intelligent) Materials

4. Introduction to Smart Materials

Smart materials, also called intelligent or responsive materials, are designed materials that have one or more properties that can be significantly changed in a controlled fashion by external stimuli, such as stress, moisture, electric or magnetic fields, light, temperature, pH, or chemical compounds. Smart materials are the basis of many applications, including sensors and actuators, or artificial muscles, particularly as electroactive polymers (EAPs).

It can divide them according to the effect of stimulation

- Piezoelectric materials
- Shape-memory alloys and shape-memory polymers
- Photovoltaic materials or optoelectronics.
- Electroactive polymers
- Magnetostrictive materials
- Magnetic shape memory

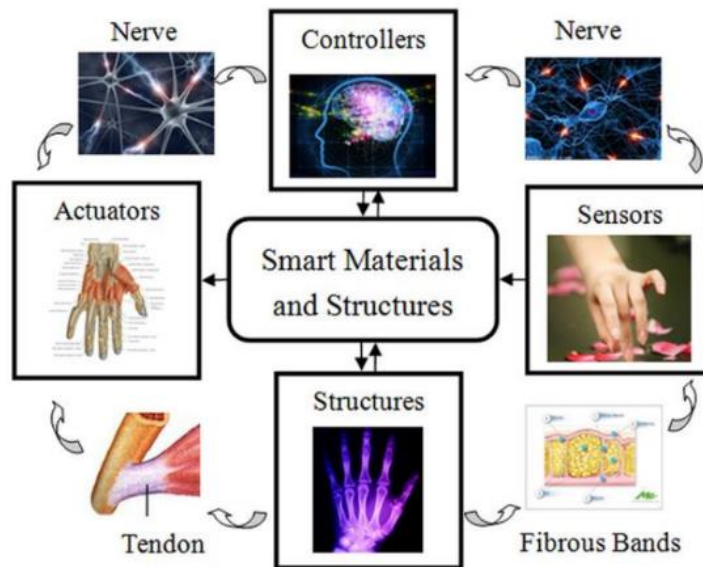


Fig.9. Smart Materials and Structures

This project has been funded with support from the Erasmus+ Programme Key Action 2 Cooperation Partnerships for Higher Education (KA220-HED). This publication [communication] reflects the views only of the authors, and the Commission cannot be held responsible for any use which may be made of the information contained therein.

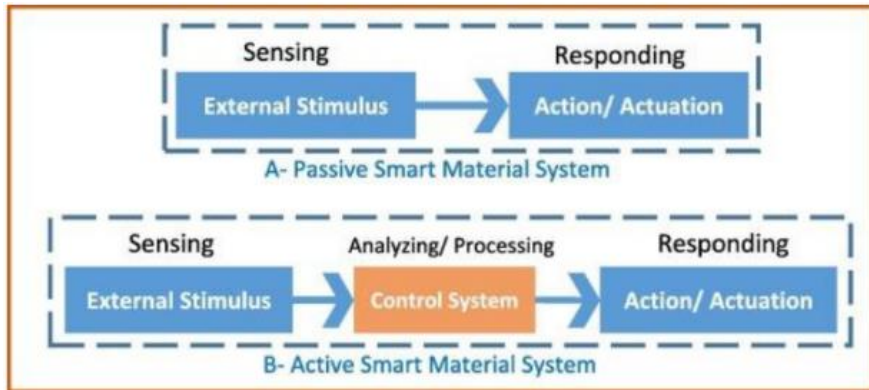


Fig.10. Smart material system

Shape Memory Alloys (SMAs)

Comparison of SMA element attached at both ends of the actuator and located outside versus inside, (b) starfish-like soft robot with flexible rays actuated by SMA spring located within the structure, and (c) spring-driven robot with a silicone polymer body (Huai-Ti and Trimmer) - Rodrigue et al., 2022, Shape Memory Alloys (SMAs).

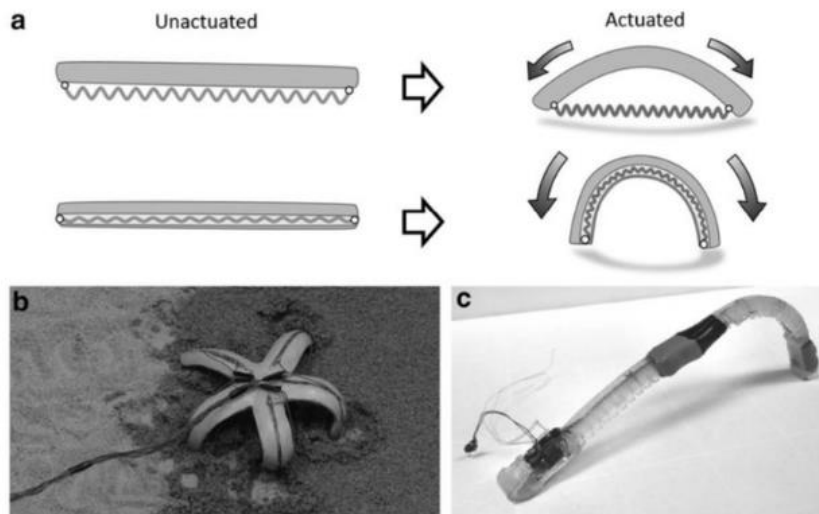


Fig.11. Shape Memory Alloys (SMAs)

This project has been funded with support from the Erasmus+ Programme Key Action 2 Cooperation Partnerships for Higher Education (KA220-HED). This publication [communication] reflects the views only of the authors, and the Commission cannot be held responsible for any use which may be made of the information contained therein.



4.1 Experiment with SMAs

In prepared E-Toolkit, an experiment was described to create a spring using Nitinol—a material known for its shape memory properties. Nitinol is an alloy of nickel and titanium that can "remember" a specific shape and return to it when heated. Through this process, a programming procedure can be carried out that allows to creation of a spring that returns to its original form after being deformed. This experiment not only demonstrates the unique characteristics of Nitinol but also helps to understand how phase transformations can influence the material's mechanical properties.



Fig.12. Fragments of Nitinol wire prepared to experiment

4.1 Process of preparing SMAs



Forming



Heating



Fast cooling

Fig.13. Process of preparing SMAs

This project has been funded with support from the Erasmus+ Programme Key Action 2 Cooperation Partnerships for Higher Education (KA220-HED). This publication [communication] reflects the views only of the authors, and the Commission cannot be held responsible for any use which may be made of the information contained therein.



4.1 Testing properties of SMAs

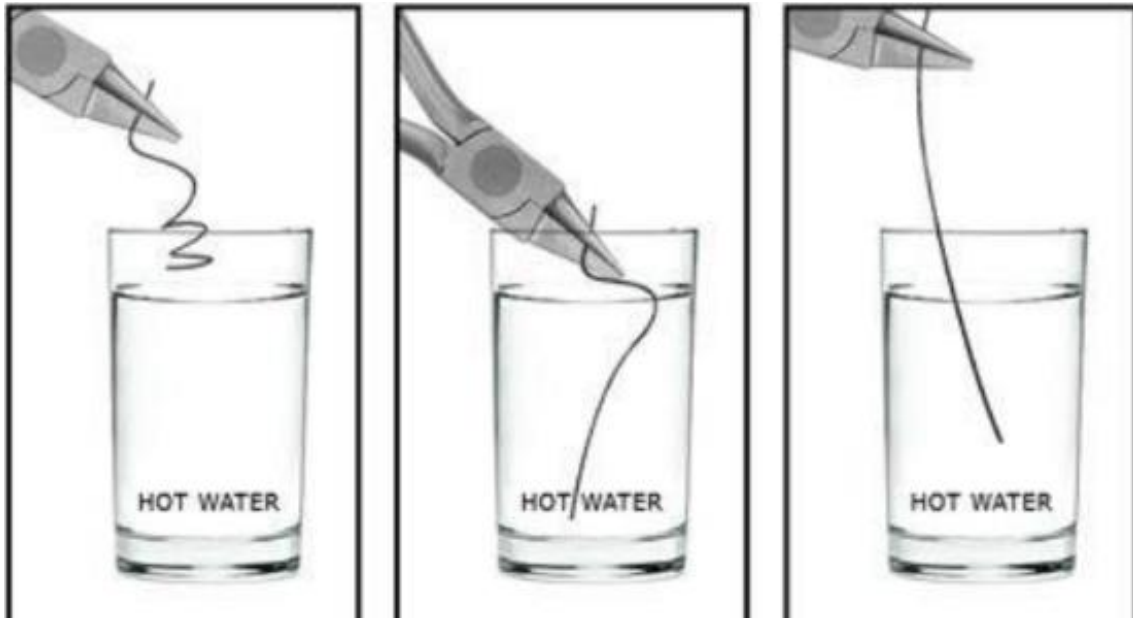


Fig.14. Testing a shape memory of a Nitinol wire

This project has been funded with support from the Erasmus+ Programme Key Action 2 Cooperation Partnerships for Higher Education (KA220-HED). This publication [communication] reflects the views only of the authors, and the Commission cannot be held responsible for any use which may be made of the information contained therein.

References

1. Autodesk. *Inventor User Guide*. Autodesk Official Website. Accessed [online](<https://www.autodesk.com/products/inventor>).
2. Zeid, I. (2014). *Mastering CAD/CAM*. McGraw-Hill Education.
3. Chua, C. K., & Leong, K. F. (2015). *3D Printing and Additive Manufacturing: Principles and Applications*. World Scientific Publishing.
4. Autodesk Knowledge Network. *Getting Started with Inventor*. Accessed [online](<https://knowledge.autodesk.com/support/inventor>).
5. Groover, M. P. (2015). *Automation, Production Systems, and Computer-Integrated Manufacturing*. Pearson Education.
6. Gorski, F., Labudzki, R., Zukowska, M., Sanfilippo, F., Ottestad, M., Zelenay, M., Băilă, D.I., Pacurar, R. *Experimental evaluation of extended reality technologies in the development of individualized three-dimensionally printed upper limb prostheses. APPLIED SCIENCES-BASEL* (2023), 13 (14), 8035. (Q1, IF 2023 = 2.5) WOS:001037958000001
7. Gorski, F., Rybarczyk, D., Wichniarek, R., Wierzbicka, N., Kuczko, W., Zukowska, M., Regulski, R., Pacurar, R., Comsa, D.S., Băilă, D.I., Zelenay, M., Sanfilippo, F. *Development and Testing of an Individualized Sensorised 3D Printed Upper Limb Bicycle Prosthesis for Adult Patients, APPLIED SCIENCES-BASEL* (2023), 13 (23), 12918. (Q1, IF 2023 = 2.5) DOI: [10.3390/app132312918](https://doi.org/10.3390/app132312918) WOS:001116054200001
8. Gorski, F., Grohs, A., Kuczko, W., Zukowska, M., Wichniarek, R., Siwiec, S., Băilă, D.I., Zelenay, M., Păcurar, R., Sanfilippo, F. *Development and studies of VR- assisted hand therapy using a customized biomechatronic 3D printed orthosis, Electronics*, vol. 13, iss. 1, 79, 2024. (Q2, IF 2023 = 2.6), DOI: [10.3390/electronics13010079](https://doi.org/10.3390/electronics13010079). WOS:001139324000001

This project has been funded with support from the Erasmus+ Programme Key Action 2 Cooperation Partnerships for Higher Education (KA220-HED). This publication [communication] reflects the views only of the authors, and the Commission cannot be held responsible for any use which may be made of the information contained therein.



Co-funded by the
Erasmus+ Programme
of the European Union



Erasmus+ Programme Key Action 2 Cooperation Partnerships for Higher Education
(KA220-HED)

Project No: 2023-1-RO01-KA220-HED-000155412

Project title: European Network for Additive Manufacturing in Industrial Design for
Ukrainian Context – Acronym: AMAZE

IO3 – AMAZE VR/AR e-learning platform for virtual laboratory

Project Title	European Network for Additive Manufacturing in Industrial Design for Ukrainian Context 2023-1-RO01-KA220-HED-000155412
Output	IO3 – AMAZE VR/AR e-learning platform for virtual laboratory
Module	Additive Manufacturing in Architecture Design
Date of Delivery	September 2024
Author	Yuriy Fedkovych Chernivtsi National University, Ukraine
Version	FINAL VARIANT, *14.09.2024

This project has been funded with support from the Erasmus+ Programme Key Action 2 Cooperation Partnerships for Higher Education (KA220-HED). This publication [communication] reflects the views only of the authors, and the Commission cannot be held responsible for any use which may be made of the information contained therein.





Co-funded by the
Erasmus+ Programme
of the European Union



Introduction

This module describes the process and structure of work in Autodesk Revit software, using the example of the reconstruction of an industrial building in Chernivtsi.

The stages of project implementation using digital technologies are described, and a 3D model of the object under study is created and printed.



Fig.1. The current condition of the brewery

1. Brief historical background

The first joint-stock brewery in Chernivtsi was built in 1869-1871. The brewery is located north of the city centre, on the right bank of the Prut River, near the railway and train station.

It was founded by local entrepreneurs Heinrich Wagner, Markus Zucker, Isaac Rubinstein and architect Gregor.



Fig.2. Historical photographs of the brewery

This project has been funded with support from the Erasmus+ Programme Key Action 2 Cooperation Partnerships for Higher Education (KA220-HED). This publication [communication] reflects the views only of the authors, and the Commission cannot be held responsible for any use which may be made of the information contained therein.





Co-funded by the
Erasmus+ Programme
of the European Union



Fig.3. Beer brands produced in Chernivtsi

Nowadays, the factory is a closed and abandoned space. The decline of this industrial building due to a number of factors has turned it into a depressed and non-functional territory. However, this building has historical and cultural value for the region. The factory's territory is located at the intersection of all major transport routes - the main arteries of Chernivtsi, which connects the site with almost all districts of the city and border the historic part of the city.

Vokzal'na Street (formerly Gagarina Street), where the factory is located, has a large daily traffic of cars and public transport from/to the historic city centre.

There is a railway station, a bus station and public transport stops close to the Research area. This indicates accessibility to the future public facility.

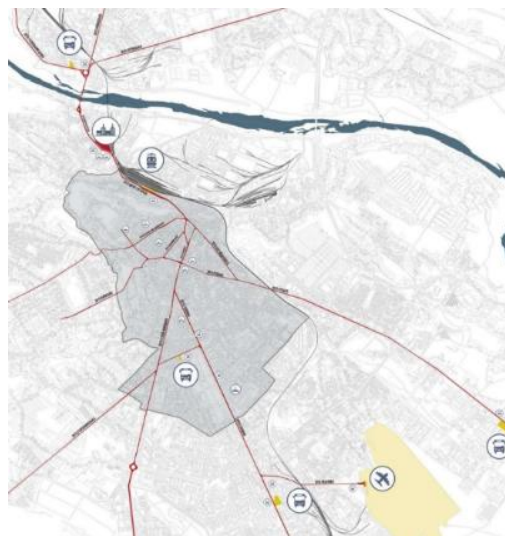


Fig.4. Situation scheme. Location of the project site in Chernivtsi

This project has been funded with support from the Erasmus+ Programme Key Action 2 Cooperation Partnerships for Higher Education (KA220-HED). This publication [communication] reflects the views only of the authors, and the Commission cannot be held responsible for any use which may be made of the information contained therein.





Co-funded by the
Erasmus+ Programme
of the European Union



Fig.5. Situation scheme. Location of the project site in Chernivtsi
Physical and architectural models of reconstruction
of an industrial building in Chernivtsi

2. Reconstruction project

The task in organising the reconstruction of this area was to create an environment that would combine and revive the surrounding existing buildings and be perceived as a single whole.

The main idea was to fit the new building into the silhouette of the old industrial neighbourhood, the chimney and the factory facade, which are present on the site.

The complex itself consists of two blocks, one historical and one modern, which contain two halls, united by a pavilion, which is a system of ramps.

For example, for large-scale conferences, presentations, and exhibitions, it is also a place for walking, with open areas with landscaping. There is also a brewery museum, which stretches over 5-floors and leads to an observation deck where visitors can enjoy the views of the city of Chernivtsi.

In general, the reconstruction of a brewery is a more environmentally friendly option for redeveloping territories than demolition and construction.

It helps to reduce the cost of reconstructing an industrial building, create the status of a cultural monument, attract additional investment in the project due to the "historical" object included in the complex, and preserve urban planning dominants.

This project has been funded with support from the Erasmus+ Programme Key Action 2 Cooperation Partnerships for Higher Education (KA220-HED). This publication [communication] reflects the views only of the authors, and the Commission cannot be held responsible for any use which may be made of the information contained therein.





Co-funded by the
Erasmus+ Programme
of the European Union



Currently, this industrial area, which has a good location near the city centre, should be allocated for commercial facilities, office centres, residential real estate and the development of the necessary infrastructure.

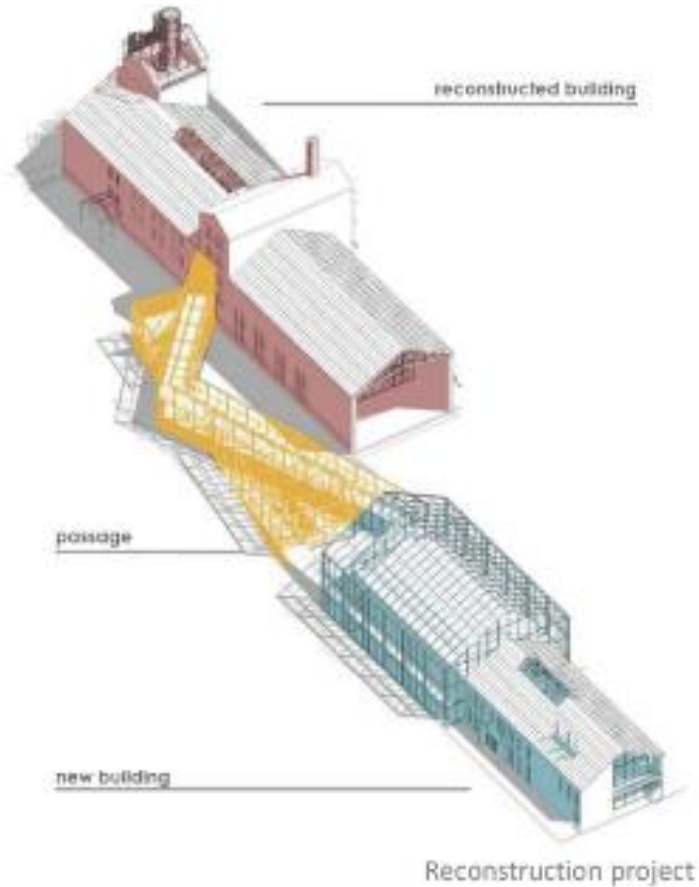


Fig.6. Reconstruction project

This project has been funded with support from the Erasmus+ Programme Key Action 2 Cooperation Partnerships for Higher Education (KA220-HED). This publication [communication] reflects the views only of the authors, and the Commission cannot be held responsible for any use which may be made of the information contained therein.





Co-funded by the
Erasmus+ Programme
of the European Union



Fig.7. Final rendering

Therefore, the reconstruction of the brewery's industrial building, and the factory's territory as a whole, in Chernivtsi, which was previously closed, is becoming a new place of attraction for the city's residents and opens up new opportunities for the reorganisation of the urban historical environment near the railway station.

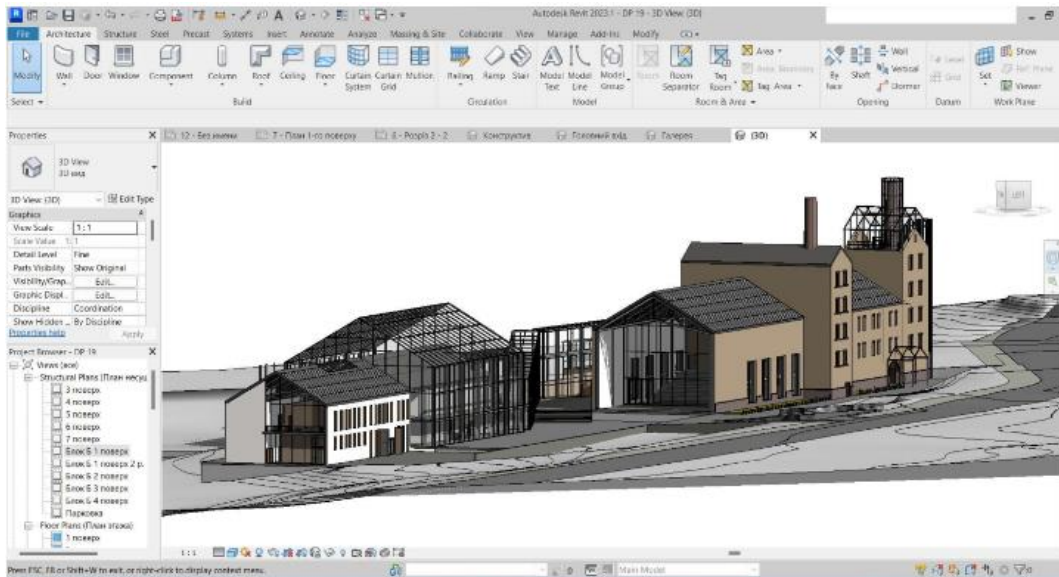


Fig.8. Elements of the Revit interface

This project has been funded with support from the Erasmus+ Programme Key Action 2 Cooperation Partnerships for Higher Education (KA220-HED). This publication [communication] reflects the views only of the authors, and the Commission cannot be held responsible for any use which may be made of the information contained therein.





Co-funded by the
Erasmus+ Programme
of the European Union

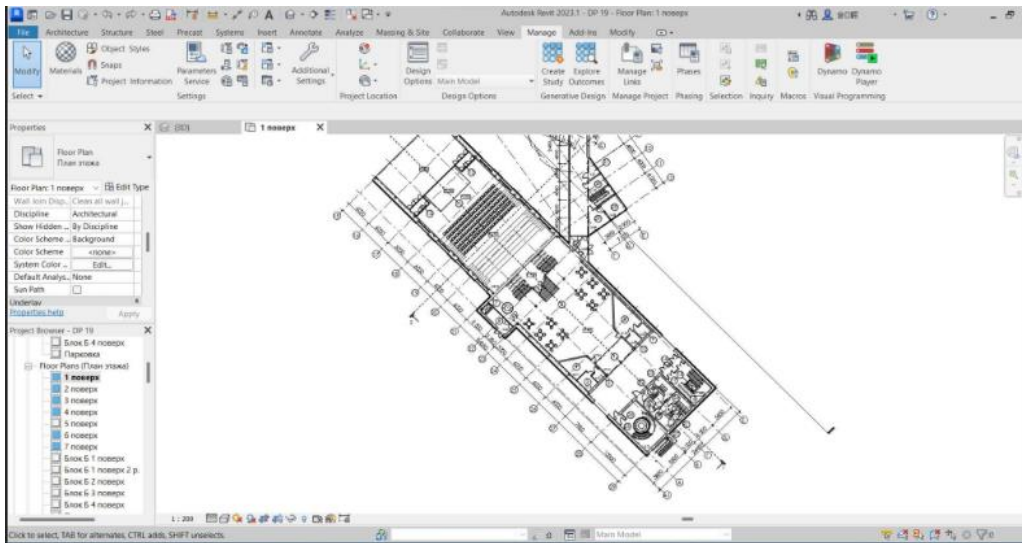


Fig.9. Axes, columns and dimensions on the plan

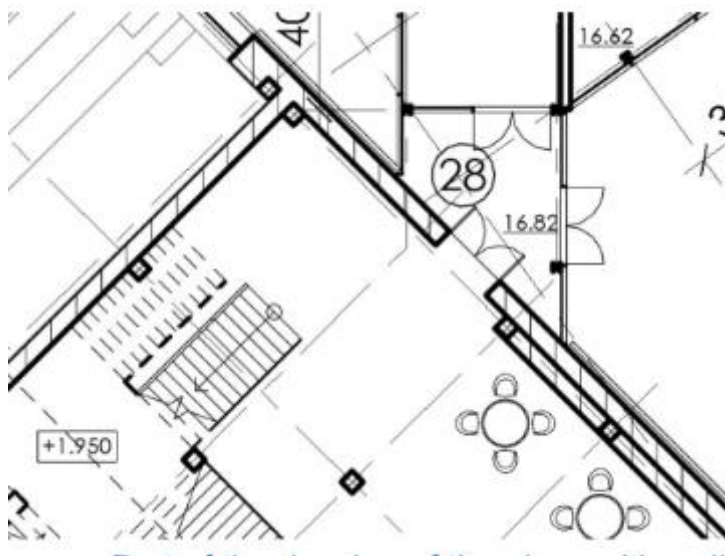


Fig.10. Part of the drawing of the plans with walls

This project has been funded with support from the Erasmus+ Programme Key Action 2 Cooperation Partnerships for Higher Education (KA220-HED). This publication [communication] reflects the views only of the authors, and the Commission cannot be held responsible for any use which may be made of the information contained therein.





Co-funded by the
Erasmus+ Programme
of the European Union

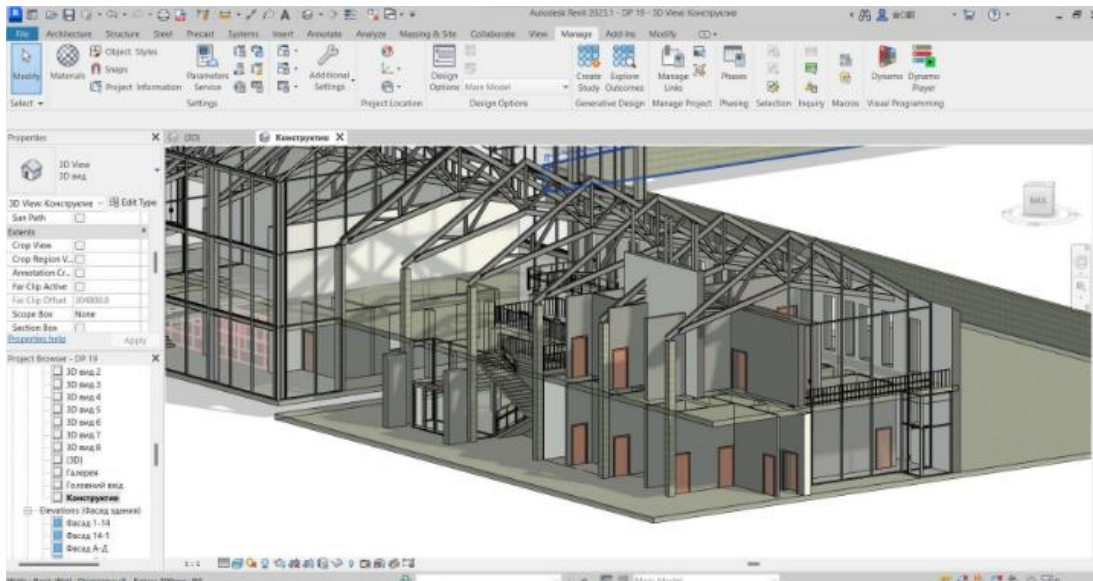


Fig.11. Design of structural elements

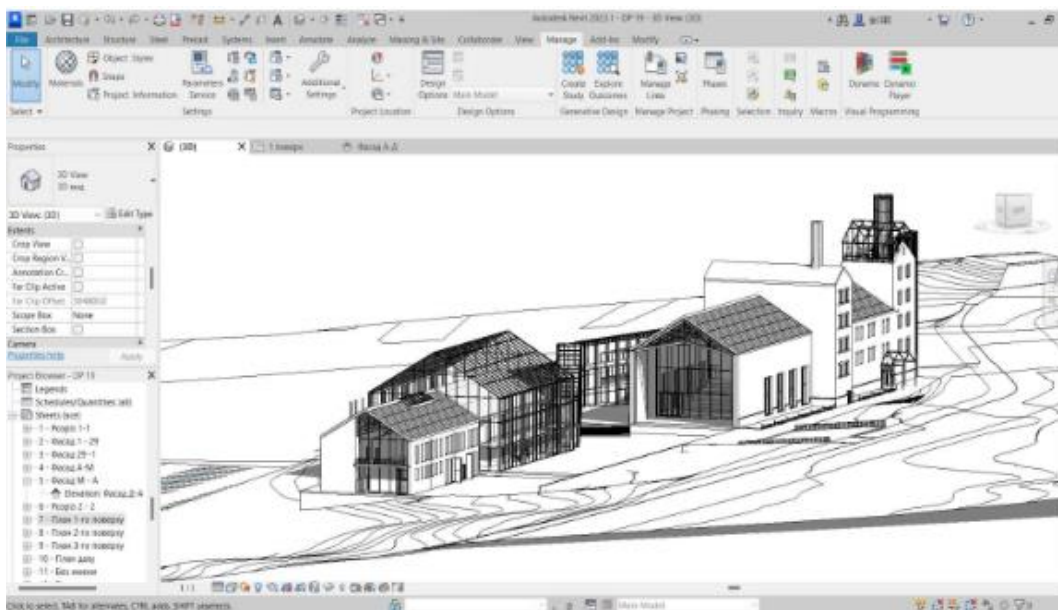


Fig.12. Hidden line style

This project has been funded with support from the Erasmus+ Programme Key Action 2 Cooperation Partnerships for Higher Education (KA220-HED). This publication [communication] reflects the views only of the authors, and the Commission cannot be held responsible for any use which may be made of the information contained therein.





Co-funded by the Erasmus+ Programme of the European Union

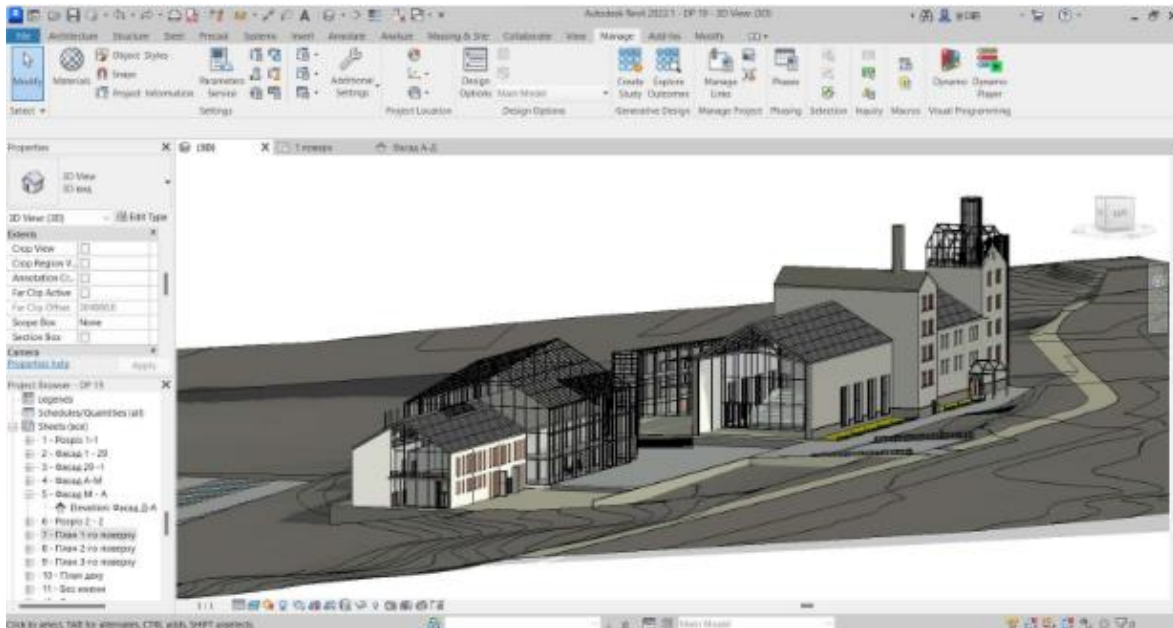


Fig.13. Realistic style

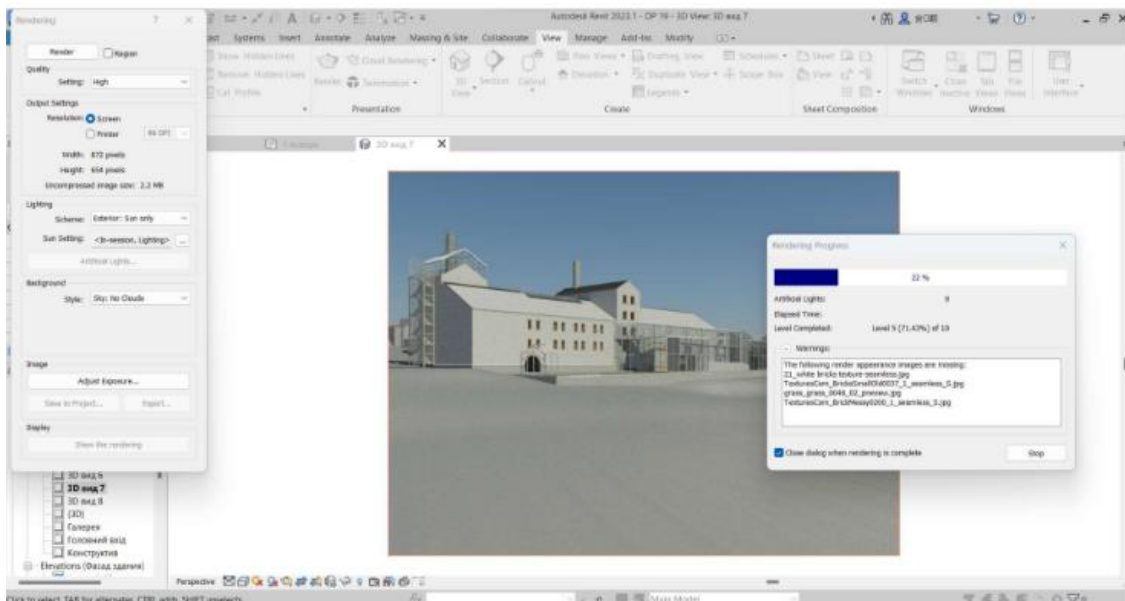


Fig.14. The rendering process in Autodesk Revit

This project has been funded with support from the Erasmus+ Programme Key Action 2 Cooperation Partnerships for Higher Education (KA220-HED). This publication [communication] reflects the views only of the authors, and the Commission cannot be held responsible for any use which may be made of the information contained therein.



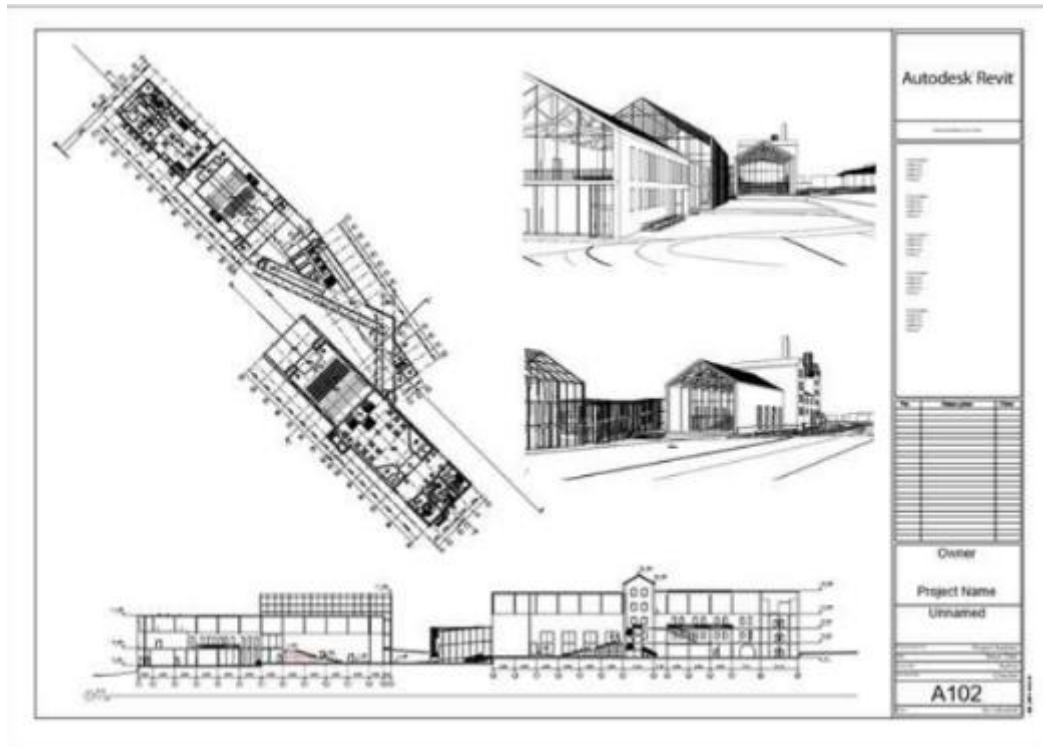


Fig.15. Completed sheet

These guidelines are aimed at learning Autodesk Revit at the level that allows to build a 3D model of a building and create basic architectural and construction drawings – plans, facades, sections. These guidelines can be used as supplementary documentation for practical training on following topics:

1. Description of the programme. Installation, interface, methods of work.
2. Setting up plan levels. Creating a grid of axes.
3. Description of walls, their characteristics.
4. Description of windows and doors, their properties. Create and configure types/styles.
5. Description of stairs and handrails, their properties. Custom shapes.
6. Description of floors and roofs. Building and editing.
7. Create a facade and section, flat and three-dimensional. Setting up the perspective view of the camera.

This project has been funded with support from the Erasmus+ Programme Key Action 2 Cooperation Partnerships for Higher Education (KA220-HED). This publication [communication] reflects the views only of the authors, and the Commission cannot be held responsible for any use which may be made of the information contained therein.



Co-funded by the
Erasmus+ Programme
of the European Union



8. Visualisation – styles, materials and light sources.

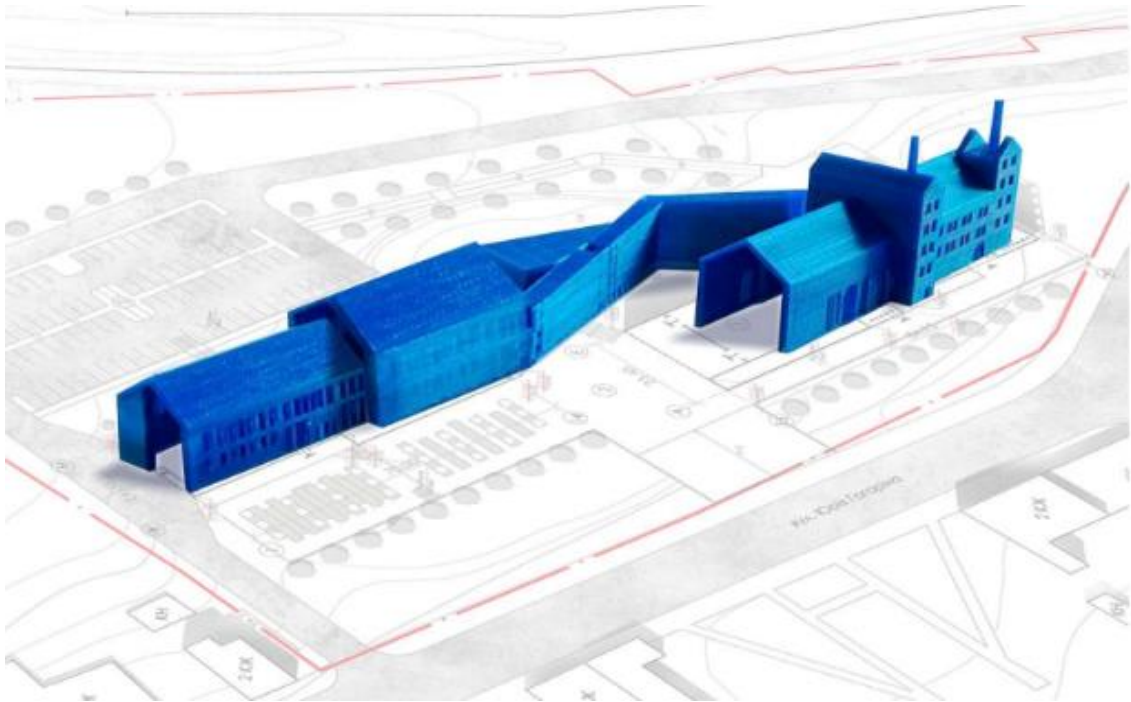


Fig.16. Printed 3D model

9. Create and design Sheets. Transfer of Views (plans, facades, sections, 3D views) to sheets.

10. Create and configure text types and sizes.

The project should provide for: development of the space-planning structure of a residential building taking into account a certain composition of premises, the author's concept, considerations of convenience, regulatory requirements for insulation, lighting, fire evacuation; selection of an appropriate structural system to ensure the stability of the building, reduce material consumption and heat loss during its operation; placement of the main and auxiliary buildings and organisation of the territory, taking into account the current planning and regulatory requirements.

It is possible to use ideas and sketches for designing a building from already finished student works.

This project has been funded with support from the Erasmus+ Programme Key Action 2 Cooperation Partnerships for Higher Education (KA220-HED). This publication [communication] reflects the views only of the authors, and the Commission cannot be held responsible for any use which may be made of the information contained therein.



3. Environment near the railway station.

Guidelines cover the creating process of a 3D model of a reconstructed brewery building in the Chernivtsi city, developed in the Autodesk Revit software, for printing on a ZMorph 2.0 SX - 3D printer with a scale of 1:500.

3.1 Project Tasks

Creating process of a 3D model using **Revit Autodesk** software [1] allows students and specialists in the architectural field to acquire the skills of:

accurate transfer of architectural objects into a digital format;

adaptation of the model to a specific scale;

preparation of the 3D model for printing, including the selection of optimal settings and the solution of possible problems arising during scaling.

These guidelines also cover the important features of preparing a file for printing, such as cleaning the model of excess details, correcting mesh errors, and selecting corresponding print settings. The printed model becomes not only a demonstration object, but also a practical tool that emphasizes the value and importance of preserving historical monuments using the digital technologies.

3.2. Equipment and Software

To perform this work, you need:

A computer with **Autodesk Revit** software installed for creating and editing a 3D model.

Software for working with STL files, such as **Meshmixer** for checking and cleaning the model.

A slicing (pre-press) program, such as **Voxelizer**, which allows you to adjust print settings and parameters.

ZMorph 2.0 SX - 3D printer that supports STL format and printing materials that provide sufficient strength and accuracy.

2. Step-by-Step Course of Work

2.1. Stage 1. Export model from Revit

Opening the project in Revit. All the necessary elements and structures must be completely finished and located in the right places. Review the placement of windows, doors, walls, and other details so that there are no extra or unnecessary elements on the model. This will help to avoid errors during printing (Fig. 17).

This project has been funded with support from the Erasmus+ Programme Key Action 2 Cooperation Partnerships for Higher Education (KA220-HED). This publication [communication] reflects the views only of the authors, and the Commission cannot be held responsible for any use which may be made of the information contained therein.



Co-funded by the
Erasmus+ Programme
of the European Union

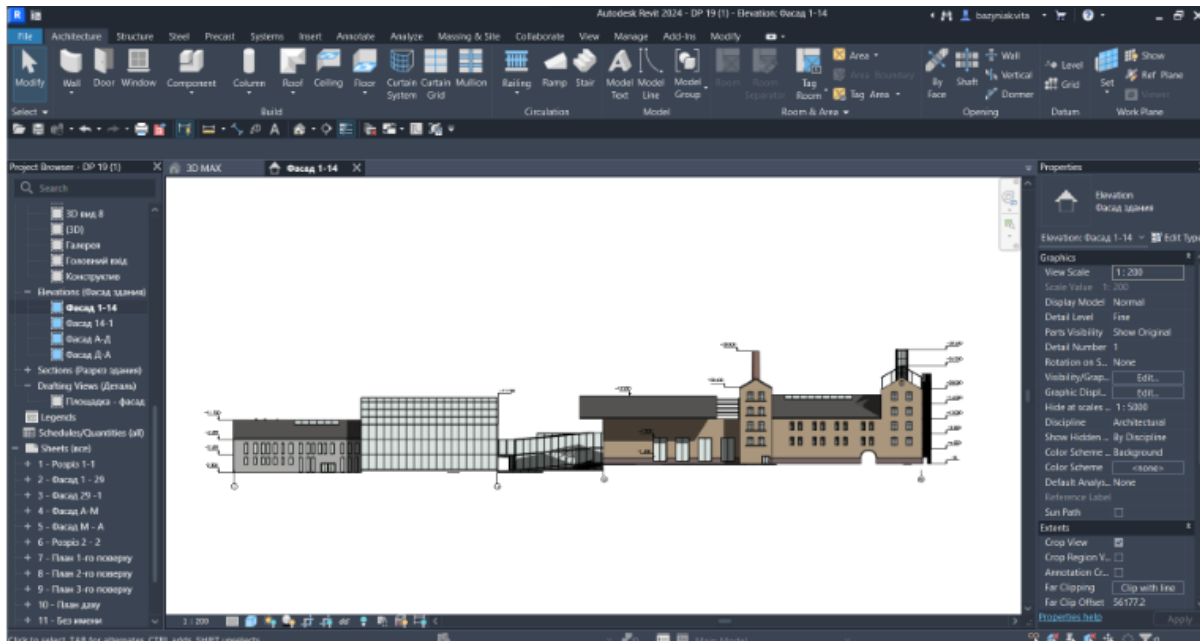


Fig. 17. Elements of the Revit interface

Preparing the model for export in 3D format. It is advisable to use special views or sections (for example, the first floor only or the exterior of the building only) to reduce the file size of the model to be printed. Some elements of the interior or engineering networks are not necessary for 3D printing, so they can be hidden or turned off. This will significantly reduce the number of polygons in the model and make it easier to processing.

Export model to STL format. Revit does not support direct export to STL format, so you need to use third-party plugins. Install the **Revit to STL** plugin via the **Autodesk App Store** [2].

After installing the plugin:

Go to the *Add-Ins* tab.

Select *Export to STL*. In the export settings, choose a scale of 1:500 (this will reduce the size of the model while maintaining the necessary proportions).

Select units of measurement. Millimetres are usually used for 3D printing, but it is important to maintain the proportionality specified in the scale.

Save the file in STL format in a convenient location on your computer. •

2.2.Stage 2. Creating STL File for Printing

This project has been funded with support from the Erasmus+ Programme Key Action 2 Cooperation Partnerships for Higher Education (KA220-HED). This publication [communication] reflects the views only of the authors, and the Commission cannot be held responsible for any use which may be made of the information contained therein.





Co-funded by the
Erasmus+ Programme
of the European Union



Checking and cleaning the model in Meshmixer or another program for working with STL files

Load the STL file into **Meshmixer**. This software allows you to clean and prepare files before printing.

Check the model for areas with poor or featureless quality:

Holes in the grid. If open surfaces or cavities are found in the model, they should be filled. In **Meshmixer**, this should be done through the **Inspector** tool.

Double surfaces and extra polygons that can reduce print quality. Delete unnecessary polygons.

If the model consists of several separate parts, they should be connected to each other into a single object via the **Make Solid** option so that the printer recognizes it as one solid object.

Scaling the model to a scale of 1:500

In **Meshmixer** or another software package, check the scale of the model. If you set the scale in **Revit**, it's worth double-checking that the model matches the selected parameters.

Adjust the zoom/scale manually if necessary. For example, **Meshmixer** has a **Transform** tool that allows you to resize the model to exact proportions .

Optimizing the model for printing

For very small model scales, like 1:500, it is worth simplifying small elements that do not play a significant role. Such details may not be reproduced on the printer, but will create an excess load

Depending on the design of the building, it may be necessary to add supports for protruding or inclined elements. This will reduce the risk of the sagging some parts of the model during 3D printing. **Meshmixer** has a tool for automatically adding supports, but sometimes it is better to add them manually taking into account the features of the model (Figures 18-21).

This project has been funded with support from the Erasmus+ Programme Key Action 2 Cooperation Partnerships for Higher Education (KA220-HED). This publication [communication] reflects the views only of the authors, and the Commission cannot be held responsible for any use which may be made of the information contained therein.



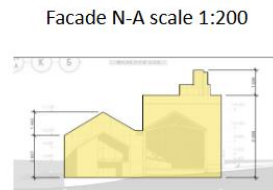
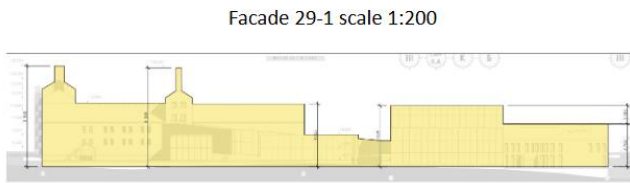
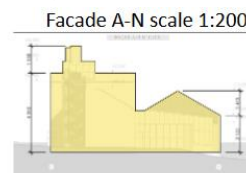
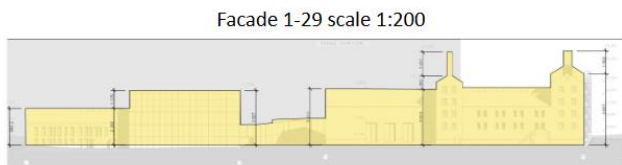
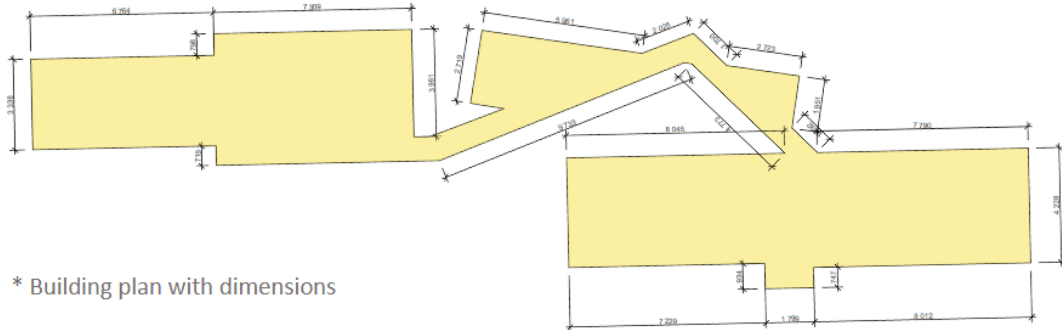


Fig.18. Building plan with dimensions

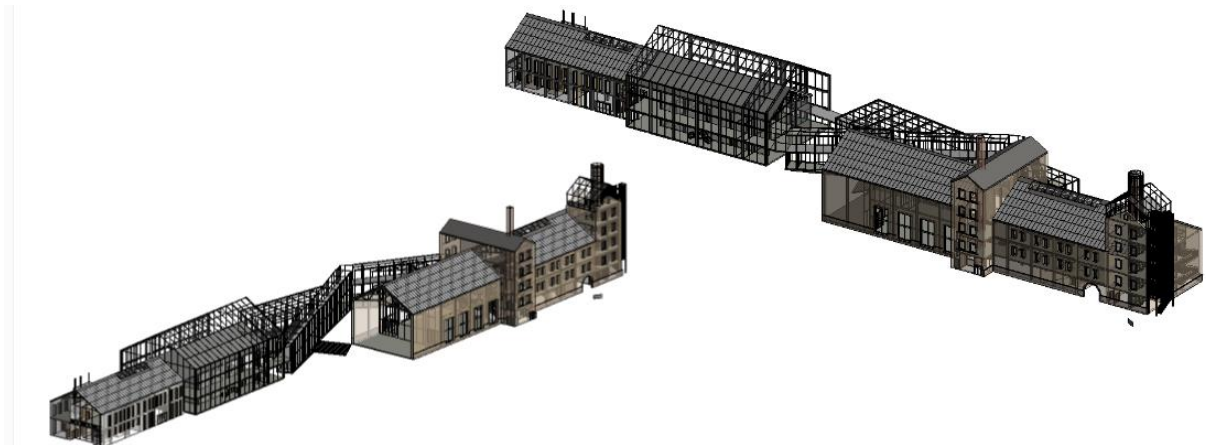


Fig.19. Design of structural elements

This project has been funded with support from the Erasmus+ Programme Key Action 2 Cooperation Partnerships for Higher Education (KA220-HED). This publication [communication] reflects the views only of the authors, and the Commission cannot be held responsible for any use which may be made of the information contained therein.



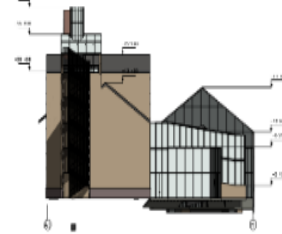
Co-funded by the
Erasmus+ Programme
of the European Union



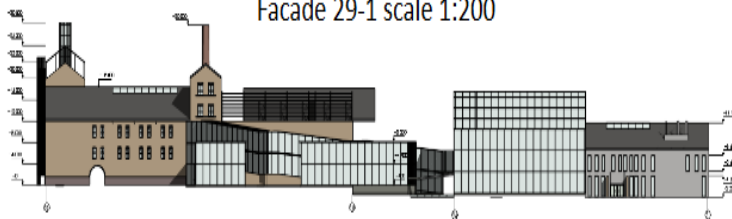
Facade 1-29 scale 1:200



Facade A-N scale 1:200



Facade 29-1 scale 1:200



Facade N-A scale 1:200

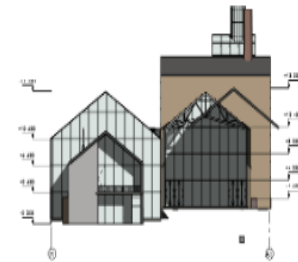


Fig.20.Hidden line style

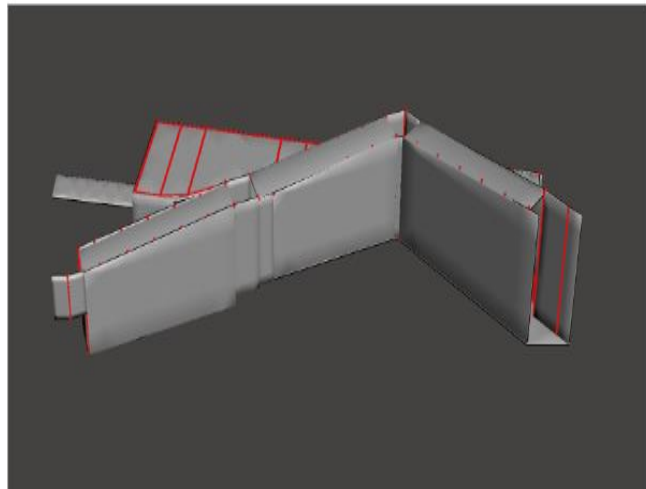
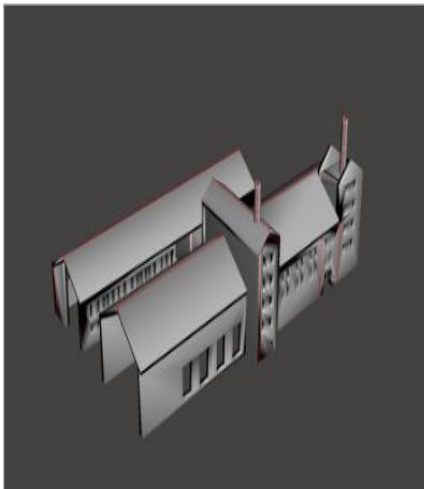


Fig. 21 Meshmixer

This project has been funded with support from the Erasmus+ Programme Key Action 2 Cooperation Partnerships for Higher Education (KA220-HED). This publication [communication] reflects the views only of the authors, and the Commission cannot be held responsible for any use which may be made of the information contained therein.





Co-funded by the Erasmus+ Programme of the European Union



Fig. 22. ZMorph 3D printer



Fig.23. Voxelizer software

This project has been funded with support from the Erasmus+ Programme Key Action 2 Cooperation Partnerships for Higher Education (KA220-HED). This publication [communication] reflects the views only of the authors, and the Commission cannot be held responsible for any use which may be made of the information contained therein.



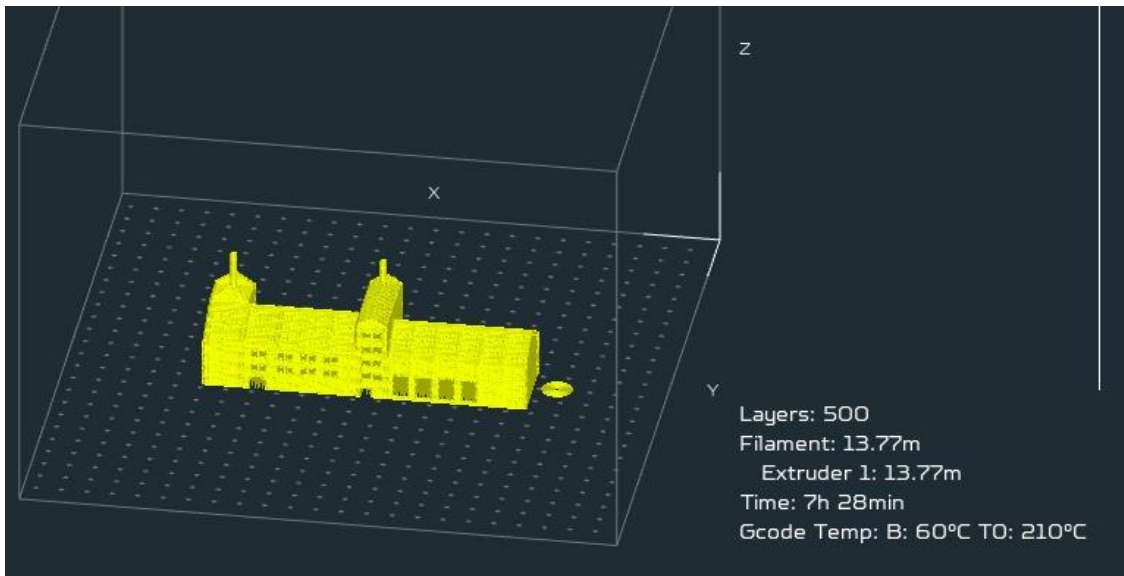


Fig.24. 3D printing parameters using Voxelizer software

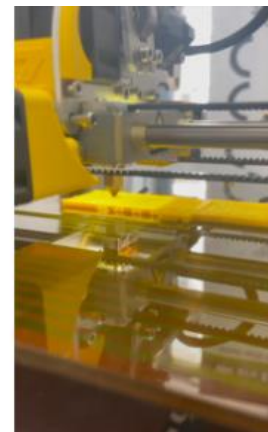
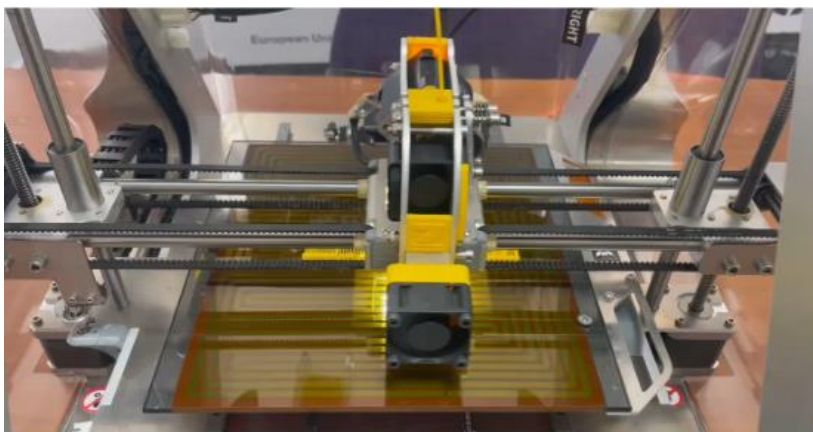


Fig.25. 3D printing process of the building prototype

Stage 3. Preparation for 3D Printing in Voxelizer, etc.

Importing the file into 3D printing software

Open **Voxelizer software**, or another platform compatible with your 3D printer. Download the STL file. You will see the model on the printer workspace, as in Figure 22

This project has been funded with support from the Erasmus+ Programme Key Action 2 Cooperation Partnerships for Higher Education (KA220-HED). This publication [communication] reflects the views only of the authors, and the Commission cannot be held responsible for any use which may be made of the information contained therein.

Adjusting the settings for 3D printing

Choose the print quality. For example:

Layer thickness: For 1:500 scale models it is recommended to set a smaller layer thickness (0.1-0.2 mm) for better detailing.

Infill: traditionally, low infill (20–30%) is assumed for building models, because exterior is more important than internal strength.

Choose the type of filament. PLA is suitable for the most architectural models, because it easily prints and has good properties.

Adjusting the model on the printing platform

Choose the orientation of the model on the printing platform. To achieve better stability and adhesion, the model is often placed with the flat surface down. This will reduce the risk of deformation during printing.

Make sure that the model fits in the printing area of the printer. Some programs have possibilities to automatically scale the model to fit on the platform, but for your work the scale should be fixed.

Preview and generation of G-code

In **Voxelizer** or another slicer, you should preview the generated print layers to see how individual model elements will look on each layer. Pay attention to intricate details or protruding elements and make sure that supports are added (if they are necessary).

After the final checking, save the G-code file on an SD card or flash card or other memory medium for transfer this file to the 3D printer (Figures. 23-24).

Stage 4. Printing Model on 3D Printer

Preparation of the 3D printer

Clean the printer platform from dust and previous filament residues.

Make sure the thread is set correctly and matches to the settings that you chose in the slicer.

Start printing

Insert the SD card into the printer or connect the printer to the computer. Download the G-code file.

Start printing and be sure to control the printing process, especially the first few layers. Correct adhesion of the model to the platform is very important, because if the initial layers detach, it can spoil the model (Fig. 25).

Completing printing

After printing is finished, give the model time to cool down to reduce the risk of model deformation and to ensure easy detachment it from the platform.

This project has been funded with support from the Erasmus+ Programme Key Action 2 Cooperation Partnerships for Higher Education (KA220-HED). This publication [communication] reflects the views only of the authors, and the Commission cannot be held responsible for any use which may be made of the information contained therein.



Co-funded by the
Erasmus+ Programme
of the European Union



Carefully remove the model from the platform using a special tool (for example, a putty knife). If necessary, remove the supports and smooth the model edges for a clean result (Fig. 24).

Stage 5. Analysis of Results

Assessment of model quality

Compare the sizes of the printed model with the initial sizes in Revit and the given scale of 1:500 (Fig. 26).

Make sure that all important details are preserved and the structure of model looks correct.



Fig. 26. The completed 3D model, which placed on the general plan. The scale is 1:500

This project has been funded with support from the Erasmus+ Programme Key Action 2 Cooperation Partnerships for Higher Education (KA220-HED). This publication [communication] reflects the views only of the authors, and the Commission cannot be held responsible for any use which may be made of the information contained therein.





Co-funded by the
Erasmus+ Programme
of the European Union



2. References

1. Autodesk Revit [Electronic resource] // Revit Architecture. Architectural design. Access mode: http://icad/software/item/autodesk_revit/;
2. Use STL Export to customize and export your Revit model to an STL file [Electronic resource]. Access mode: <https://help.autodesk.com/view/RVT/2024/ENU/?guid=GUID-93AE8701-3958-43E9-8D95-0C1650B88061>
3. Autodesk [Electronic resource]. Architectural design and construction of buildings. Access mode: <https://www.autodesk.ru/products/revit-family/case-studies/architectural-design>

This project has been funded with support from the Erasmus+ Programme Key Action 2 Cooperation Partnerships for Higher Education (KA220-HED). This publication [communication] reflects the views only of the authors, and the Commission cannot be held responsible for any use which may be made of the information contained therein.

